Part II
Eyespots and Evolution

Chapter 5
Physiology and Evolution of Wing Pattern Plasticity in *Bicyclus* Butterflies: A Critical Review of the Literature

Antónia Monteiro

Abstract Phenotypic plasticity refers to the ability of a genotype to develop into different phenotypes in response to environmental cues. In many instances, this ability is an evolved adaptation to enable organisms to adapt to predictable but variable environments in time or space (West-Eberhard MJ, Developmental plasticity and evolution. Oxford Unversity Press, New York, p 794, 2003; Stearns SC, BioScience 39(7):436–445, 1989; Bradshaw AD, Evolutionary significance of phenotypic plasticity in plants. In: Caspari EW (ed) Adv Genet 13. Academic, New York, pp 115–155, 1956; de Jong G, New Phytol 166(1):101–117, 2005; Moran NA, Am Nat 139(5):971–989, 1992). While much research has focused on the ecological and adaptive significance of the alternative phenotypes produced under different environments, relatively little is still known about the proximate physiological and molecular mechanism translating environmental variation to phenotypic variation and how these mechanisms may have evolved (Beldade P, Mateus ARA, Keller RA, Mol Ecol 20(7):1347–1363, 2011).

Here I provide a review of the literature that has explored how environmental variation, in particular seasonal variation, impacts eyespot size in African satyrid butterflies of the genus *Bicyclus*. Plasticity in eyespot size is undeniably the most conspicuous effect of seasonal variation on the appearance of *Bicyclus* species, and perhaps because of this, its ecological and physiological bases have been under investigation since 1984 (Brakefield PM, Reitsma N, Ecol Entomol 16:291–303, 1991; Brakefield PM, Larsen TB, Biol J Linn Soc 22:1–12, 1984). Much subsequent research on members of this genus, and in particular on the model species *Bicyclus anynana*, uncovered, however, many other morphological, behavioral, physiological, and life history traits that are equally impacted by seasons and, in particular, by rearing temperature (Bear A, Monteiro A, Plos One 8(5), 2013; Dion E, Monteiro A, Yew JY, Scientific Reports 6:39002, 2016; Fischer K, Brakefield PM, Zwaan BJ, Ecology 84(12):3138–3147, 2003a; de Jong MA, Kesbeke F,

A. Monteiro (✉)
Department of Biological Sciences, National University of Singapore, 117543 Singapore, Singapore

Yale-NUS College, 138609 Singapore, Singapore
e-mail: antonia.monteiro@nus.edu.sg

Brakefield PM, Zwaan BJ, Climate Res 43(1–2):91–102, 2010; Mateus ARA, Marques-Pita M, Oostra V, Lafuente E, Brakefield PM, Zwaan BJ, et al. Bmc Biology 12, 2014; Windig JJ, Brakefield PM, Reitsma N, Wilson JGM, Ecol Entomol 19:285–298, 1994; Fischer K, Eenhoorn E, Bot AN, Brakefield PM, Zwaan BJ, Proc R Soc B 270(1528):2051–2056, 2003b; Everett A, Tong XL, Briscoe AD, Monteiro A, BMC Evol Biol 12:232, 2012; Prudic KL, Jeon C, Cao H, Monteiro A, Science 331(6013):73–75, 2011; Westerman E, Monteiro A, Plos One 11(2), 2016; Macias-Munoz A, Smith G, Monteiro A, Briscoe AD, Mol Biol Evol 33(1):79–92, 2016). This review, however, focuses solely on eyespots, the original trait that initiated explorations of phenotypic plasticity in this butterfly genus.

Keywords Plasticity • Eyespots • 20-Hydroxyecdysone • Hormone manipulations • Cucurbitacin • Temperature • Developmental plasticity • Sexual ornaments

5.1   Introduction

Insects have relatively short lives, and this promotes the evolution of seasonal forms or polyphenisms. A short life means that insects can live all their lives within a particular season, in regions of the world that have seasons. This also means that cohorts that emerge in different seasons (spring or summer or wet or dry seasons) will encounter very different biotic and abiotic environments. These environments often exert different selection pressures on the appearance of these insects in order to enhance their survival and reproduction in the respective season. The evolution of adaptive phenotypic plasticity is then a natural response to these predictable, recurrent, but alternate environments that different cohorts of insects experience at different times of the year. This type of plasticity is called a seasonal polyphenism and is especially notable in the highly conspicuous wing patterns of butterflies that inhabit seasonal environments (Brakefield and Larsen 1984; Nijhout 1999, 2003).

   One type of wing pattern in butterflies that is especially sensitive to seasonality is the eyespot pattern. Eyespots found in the exposed surfaces of the wings (most of the ventral wing surfaces) are often large in the wet season (WS) and small in the dry season (DS) in the African tropics (Brakefield and Larsen 1984), as well as in many other regions of the world (Fig. 5.1). The ecological significance of this plasticity has been explored with a variety of experiments in the field (Brakefield and Frankino 2009; Ho et al. 2016) and in the lab (Lyytinen et al. 2003, 2004; Prudic et al. 2015; Olofsson et al. 2013; Vlieger and Brakefield 2007). The consensus, so far, is that small cryptic eyespots are an adaptation of the butterfly to avoid being detected by vertebrate predators, who predominate in the DS (Lyytinen et al. 2003), whereas the more conspicuous eyespots are an adaptation to deflect the attacks of invertebrate predators, such as mantids, who predominate in the WS (Prudic et al. 2015).
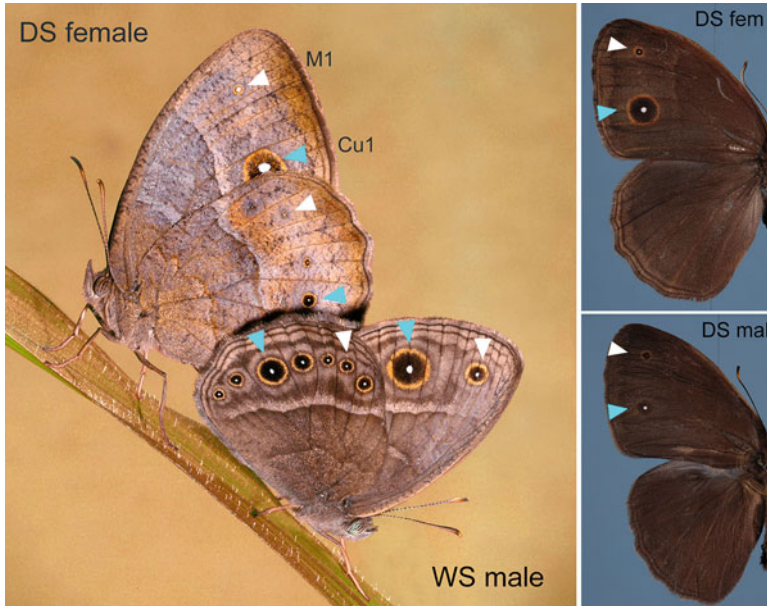
Fig. 5.1 Patterns of plasticity in *Bicyclus anynana* butterflies. Main image depicts a DS female (*left*) mating with a WS male. Eyespots described in this review are named M1 (*white arrow*) and Cu1 (*blue arrow*). The ventral wing surfaces are often exposed to predators with the exception of the Cu1 forewing eyespot, which is often hidden by the hindwing. The *right panels* depict the hidden (*dorsal*) surfaces of a DS female (*top*) and a DS male displaying sexual dimorphism in their Cu1 eyespots

Butterfly eyespots that are found in hidden (mostly dorsal) surfaces have different patterns of plasticity altogether because these eyespots serve different functions in each of the seasons. These eyespots are used in sexual signaling by both sexes (Prudic et al. 2011; Robertson and Monteiro 2005; Costanzo and Monteiro 2007) (Fig. 5.1). Males use these eyespots to signal to females in the WS, and females use the same eyespots to signal to males in the DS. This leads to patterns of size plasticity that are congruent with those from ventral surface eyespots for males (large in WS males and small in DS males) but not for females. DS females, in particular, have abnormally large dorsal eyespots, which they use for sexual signaling to males in this season (Fig. 5.1), which are at odds with the small size of their ventral exposed counterparts. Females, thus, don't display size plasticity in these eyespots – they are large in both seasons. The patterns of sexual selection operating on dorsal eyespots lead to sexual size dimorphism in dorsal Cu1 eyespots in the DS (Fig. 5.1), as well as a male-specific pattern of plasticity for these eyespots (Bhardwaj et al. 2017).

The review that follows looks critically at the literature that has investigated the environmental, physiological, and molecular mechanisms that regulate eyespot size plasticity in both dorsal and ventral eyespots. In addition, the evolution of phenotypic plasticity in eyespot size is also reviewed.

5.2   Physiological Mechanisms of Eyespot Plasticity

Bicyclus anynana is found from Ethiopia to South Africa (Condamin 1973) and has evolved along a range of climates, but the original lab population of *Bicyclus anynana* stems from Malawi, a country with strong seasonality. The arrival of the dry season in Malawi is primarily cued by decreasing temperatures, whereas the arrival of the wet season is cued by increasing temperatures (Brakefield and Reitsma 1991). Lab-rearing experiments, where photoperiod and thermoperiods were varied, confirmed that average temperature and fluctuations in night- and daytime temperature were the most important determinants of eyespot size plasticity in this species (Brakefield and Mazzotta 1995). Food plant quality, however, also affected eyespot size plasticity (Kooi 1995).

Once environmental cues with significant effects on the induction of plasticity were identified, the next investigations probed how and when these cues interacted with the gene regulatory networks that differentiate the eyespot patterns to modify their output in a plastic manner. In particular, these investigations focused on the mechanisms whereby average daily temperature induced the wet and the dry seasonal forms in *B. anynana*.

The first consideration was whether temperature only exerted its effects on wing pattern development during specific developmental windows or critical temperature-sensitive stages. Early work in this system used temperature-shift experiments to identify the critical period during eyespot development that was sensitive to rearing temperature and able to modify the final size of eyespots (Kooi and Brakefield 1999). These experiments used a variety of shifts differing in length of time that the animals were kept at each of the two alternative temperatures (17 and 27 °C) and times of initiation of the shift. Kooi and Brakefield (1999) concluded that the most important period of sensitivity that led to changes in the size of two of the ventral eyespots (forewing M1 and hindwing Cu1 eyespots) was the final 5th larval instar. Furthermore, while they found that temperatures experienced during the first 24 hrs of pupal development still impacted eyespot size, they concluded that temperatures experienced during this period could not shift a WS wing pattern into a DS pattern and vice versa (Kooi and Brakefield 1999).

More recent work replicated these experiments, with narrower window temperature shifts, and confirmed that the late larval period, in particular, the wandering stage of development, when the larvae stop eating and start looking for a place to pupate, was the most temperature-sensitive stage for the determination of ventral eyespot size plasticity of Cu1 ventral hindwing eyespots (Monteiro et al. 2015). These experiments also highlighted that forewing and hindwing ventral Cu1 eyespots in females responded differently to temperature. Forewing Cu1 eyespots, which are normally hidden by the hindwing when the butterfly is at rest (Fig. 5.1), were much less plastic than Cu1 hindwing eyespots, which are always exposed at rest. In addition, the size of the white center in forewing eyespots was not plastic at all (Monteiro et al. 2015). Subsequent work (Bhardwaj et al. 2017), examining plasticity in dorsal eyespots, similarly concluded that the wandering

stage is the most temperature-sensitive stage for male eyespots (female eyespots are not plastic). In summary, eyespot size is primarily sensitive to temperature during the wandering stages of development, but size of Cu1 serial homologous eyespots on ventral forewings and hindwings does not respond to temperature in the same way.

Most examples of phenotypic plasticity known from insects seem to rely on a hormonal signal to translate variable environments into variable phenotypes (Nijhout 1999, Beldade et al. 2011). This prompted the search for the hormones responsible for the variation in wing pattern across *B. anynana* seasonal forms. Previous work on two different butterflies, the map butterfly *Araschnia levana* and the buckeye *Junonia coenia*, had discovered that differences in the presence and absence of a peak of the molting hormone, 20-hydroxyecdysone (20E), during the early pupal stage explained the different seasonal forms (spring and summer forms) of these butterflies, displaying different wing colors in response to day length (an important environmental cue used for regulating plasticity in these systems) (Koch and Buckmann 1987; Nijhout 1980; Rountree and Nijhout 1995). 20E became, thus, a candidate hormone to be investigated in connection with eyespot size plasticity in *B. anynana*.

Surprisingly, early work surrounding investigations into the physiological basis of eyespot size plasticity decided not to investigate physiological differences between the seasonal forms but instead focus on physiological differences observed between lines reared at the intermediate temperature of 20 °C, whose eyespots had been artificially selected to mimic the dry and wet season forms (Brakefield et al. 1998; Koch et al. 1996). In addition, titers of 20E were measured in individuals of these WS and DS form "genetic mimics" at different stages of development focusing primarily in the early pupal stages, as no differences were observed between these mimics during the wandering stages (Koch et al. 1996). Titers of 20E measured in the early pupal stage showed small differences between the seasonal form genetic mimics, and 20E injections into the dry season form mimic, which had a natural slower increase of 20E during the pupal stage, showed small (albeit significant) increases in eyespot size toward the phenotype of wet season forms (Koch et al. 1996). Later work, however, showed that these 20E titer differences observed between WS and DS form genetic mimics could more readily explain variation in pupal stage duration than eyespot size differences (Oostra et al. 2011).

Recent work finally measured 20E hemolymph titers in late larvae of temperature-induced WS and DS forms and discovered that levels of 20E differed significantly between the seasonal forms during the wandering stage of development (Monteiro et al. 2015). This is important because this stage of larval development is contained within the 5th and final larval stage, previously identified as the temperature-sensitive period for induction of eyespot size plasticity (Kooi and Brakefield 1999; Monteiro et al. 2015). Levels were higher in WS forms relative to DS forms, indicating a positive correlation between 20E and eyespot size.

To test whether these different levels in 20E were causing the variable wing phenotypes, hormone injections and hormone receptor manipulations were both

done. These two types of manipulations, however, are not equivalent, but this has remained unrecognized by many researchers in this field (but see Zera 2007). To test whether the presence of a hormone at a given level is leading to the development of a phenotype, removal of the hormone or its producing cells/organs, or interfering with its specific receptor, are the best type of manipulations to test causation. If this cannot be done, adding hormone to the form with the lower natural levels to mimic the form with the highest levels is also possible. This latter type of manipulation, however, is more challenging to do because levels of the added hormone need to mimic rather than exceed the highest natural levels found in any of the plastic forms. If levels exceed the natural levels, this may lead to abnormal phenotypes that play no role in normal trait development. One way these abnormal phenotypes may emerge is if raising the levels of hormone A beyond some critical level stimulates the production of hormone B, which then impacts the trait of interest directly. In this situation, manipulations of hormone A would lead researchers to conclude incorrectly that it regulates the trait, when in fact it does so only via its effects on hormone B, which was induced due to high abnormal levels of A. Cross talk between hormonal systems is common, and special attention needs to be paid to this (Zera 2007; Orme and Leevers n.d.).

An example of the type of asymmetry in the response that can be observed with the two types of manipulation experiments described above was observed with 20E signal manipulations in the wandering larval stages of *B. anynana*. As mentioned above, WS wanderers have higher levels of 20E relative to DS wanderers. In order to test whether 20E levels at this stage of development were regulating adult eyespot size, injections of cucurbitacin B (CurcB), a EcR receptor antagonist (Dinan et al. 1997), and a control vehicle, were performed in WS wanderers to test whether they led to reduced adult eyespot size (Monteiro et al. 2015). CurcB is a small molecule that binds with high affinity to the ecdysone receptor (EcR), preventing 20E from binding it and preventing downstream signaling from taking place (Dinan et al. 1997). Injecting CurcB into WS forms led to adult butterflies exhibiting small eyespots resembling DS forms (Monteiro et al. 2015). However, Cu1 ventral forewing eyespots, which are less plastic than their Cu1 ventral hindwing counterparts, did not change in size. The asymmetry in the response of the two Cu1 eyespots to CurcB injections can be explained because the EcR receptor is present in Cu1 forewings eyespot centers but is absent in Cu1 hindwing eyespot centers (Monteiro et al. 2015). Absence of the receptor in forewing eyespot centers essentially makes them insensitive to the CurcB manipulation. What is important to note, however, is that these forewing eyespots, despite expressing no EcR, responded to injections of 20E and increased in size, just like their hindwing counterparts that expressed EcR. One possibility is that if 20E levels attained in DS forms via injections were beyond those observed in WS forms, they may have stimulated the production of a second hormone, which also contributed to the regulation of hindwing eyespot size via its own receptor.

To understand how temperature (and hormones) affected eyespot development, Brakefield et al. (Brakefield et al. 1996) looked at an early marker of eyespot development, the transcription factor *Distal-less (Dll)*, in late larvae and in early

pupae. Dll showed comparable expression domains in 5th instar larval wings but had a broader domain of expression in the eyespot centers of WS forms in the early pupal stage. In addition, this gene also had a second domain of expression that corresponded to the much broader black disc of scales in an eyespot, which became visible later, around 12 h after pupation (Brunetti et al. 2001a; Monteiro et al. 2006). The larger group of cells expressing Dll clustered in the eyespot center, however, suggested that some time in between the late larvae and early pupal stages, the eyespot centers were becoming larger in response to temperature. A subsequent study looked at two other markers for eyespot development and found that Notch and Engrailed genes were expressed earlier in the eyespot centers of DS forms relative to their later expression in WS forms, suggesting that these genes could be downregulating eyespot size in DS forms (Oliver et al. 2013). The onset of Dll expression in the eyespot centers of WS and DS forms, however, was approximately the same (Oliver et al. 2013). A more recent study (Bhardwaj et al. 2017) showed that a fourth gene expressed in eyespot centers, the ecdysone receptor (EcR), showed an enlargement in its domain of expression during the second half of the wandering stage in WS forms. Cells in the center of dorsal forewing eyespots underwent cell division concurrently with the rise of 20E titers taking place at that stage of development. Other marker genes, such as Spalt, also increased their domains of expression at the same time, concurrently with local cell divisions. Cells in the dorsal eyespot centers of DS males, however, experiencing the lowest levels of 20E hormone, did not undergo cell division and produced a small eyespot center as well as an associated small eyespot. To test whether levels of 20E were directly responsible for the regulation of dorsal eyespot center size via a localized process of cell division, injections of 20E (into DS males) and CurcB (into WS forms) at 60% of wandering stage development were performed and confirmed an effect of 20E levels on the regulation of eyespot center sizes in WS individuals as well as in DS females, the odd sex with the abnormally large eyespots (Bhardwaj et al. 2017).

The experiments above pin the critical stage of regulation of eyespot center size, and eyespot size for both dorsal and ventral eyespots, to the second half of the wandering stage of development. At this stage, rearing temperature leads to variation in 20E titers, which in turn leads to localized patterns of cell divisions in cells that express the EcR receptor (Bhardwaj et al. 2017). These localized patterns of cell division determine the size of the eyespot centers, which are critical determinants of the size of the complete eyespot pattern (Monteiro and Brakefield 1994), and thus impact final eyespot size.

For many years, however, research into the physiological and genetic basis of eyespot size plasticity focused exclusively on the period of development following pupation, which is not as sensitive to temperature as the previous larval wandering stage (Kooi and Brakefield 1999; Monteiro et al. 2015). This period shows variation in timing of 20E titers in the seasonal form "genetic mimics" as well as in the actual seasonal forms (Mateus et al. 2014; Oostra et al. 2011). In particular, titers of 20E are low during the first 24 h (WS) (and 48 h in the DS) after pupation, which is the developmental window believed to be important for eyespot ring differentiation at

high temperatures (French and Brakefield 1992; Brunetti et al. 2001b). This period of low hormone titers is followed by steadily rising 20E titers, where titers raise earlier in WS than in DS forms, relative to total development time. Furthermore, injections of large quantities of 20E (0.1 ug) into young pupae (0–6 h old) reared at 20 °C led to no changes in eyespot size (Koch et al. 1996). Eyespot size changed slightly only with injection of 20E doses larger than 0.25 ug at this early pupal stage (Koch et al. 1996). Note that injections of merely 0.006 ug of 20E (a dose that is 16 times smaller than 0.1 ug) into wanderers reared at 17 °C were sufficient to produce an almost complete seasonal form reversal in this butterfly species (Monteiro et al. 2015).

More recent experiments, focusing again on the early pupal stage, remeasured 20E titers in vehicle-injected and 20E-injected young pupae (3% of pupal development) reared at two different temperatures (19 and 27 °C) and documented small but significant differences in 20E hormone titers between vehicle-injected seasonal forms right after the injections (at 3.5% of pupal development) (Mateus et al. 2014). WS forms had slightly higher titers of 20E than DS forms. Differences in 20E titers in vehicle-injected seasonal forms, however, were no longer present at 8% of pupal development. While these titer measurements are not exactly "baseline" measurements for natural levels of 20E across these two rearing temperatures, they nevertheless show differences in 20E levels across the two seasonal forms (Mateus et al. 2014). In order to test the significance of these differences, injections of 20E were performed into both DS and WS seasonal forms at this early stage (3%) of pupal development, as well as at a later stage (16% pupal development), before the large raise in 20E titers. Special attention was paid to changes in the area of each of the color rings (white center, black, and gold ring) in a variety of different eyespots on dorsal, ventral, forewing, and hindwing surfaces, which are being determined at this stage of development (Brunetti et al. 2001b). One point of concern in these experiments, however, is that injections used 0.25 ug of 20E, a dose previously shown to produce effects on ventral wing patterns (Koch et al. 1996) but also shown to lead to unnaturally high levels of 20E titers in the hemolymph of pupae of both seasonal forms at both 3.5 and 8.5% development (Mateus et al. 2014).

These hormone manipulations showed that early (3%), but not later (16%), injections led to a variety of phenotypes. In particular, they affected the area of some of the color rings, of some of the eyespots, on some of the wing surfaces. When expression of EcR was examined across these different wing pattern traits, there was no clear correlation between the traits affected and the presence/absence of EcR expression in that trait (Mateus et al. 2014). It is possible that, as in the injection experiments performed during the wandering stage of development, these injections are stimulating a second hormonal system, which in turn is exerting its effects on the eyespot phenotypes via its own receptor. Alternatively, given that only those eyespots and eyespot traits that were shown to be especially plastic responded to the hormone injections, it is possible that 20E is regulating directly the expression of these traits, but the developmental stage examined only captures effects on individuals with extended periods of sensitivity or heightened sensitivity to the hormone. Alternatively, lower basal levels of EcR observed across the whole

pupal wing epidermis are all that is required for 20E signaling to function at the period of development examined. None of the dorsal eyespots, however, responded to the injections (Mateus et al. 2014). This is likely because dorsal eyespot size plasticity, just as ventral eyespot size plasticity (Monteiro et al. 2015), is primarily controlled during the wandering stages of development (Bhardwaj et al. 2017), but perhaps these dorsal eyespots have fewer hormonal systems controlling their development, and cross talk between hormonal systems may have been minimized.

Going forward, future work on the physiological and genetic basis of wing pattern plasticity in any butterfly species should pay attention to a successive series of experiments that progressively narrows down the causative elements of trait plasticity. First, the critical period in development that is responsible for inducing trait plasticity should be identified using shifting experiments (see Monteiro et al. 2015). It is important to study each trait independently and not assume that the window of development controlling the features of a specific trait (say black ring of M1 eyespot on ventral forewing surface) will be the same as that controlling a similar but not identical trait (e.g., white center of the Cu1 eyespot on a different wing surface). Second, the physiological differences present at that stage (not later and not earlier) should be examined to pin down the physiological correlates that may underlie differences in trait development. Third, hormone depletion experiments (first) and hormone addition experiments (second) should be performed in order to mimic the physiological state of the two plastic forms, in a way that is independent of the environmental cue, to test causation. Here it is especially important to not raise hormone levels above those actually observed in the natural forms in order to avoid stimulating other hormone signaling systems in abnormal ways.

5.3 Evolution of Plasticity

Experiments on the evolution of plasticity in *B. anynana* have been of two types: microevolutionary population-level studies and macroevolutionary species-wide comparative studies. I will review these two types of experiments in turn.

The first type of study focused on testing whether genetic variation controlling the slope of a reaction norm, i.e., the sensitivity of ventral eyespot sizes to rearing temperature, was present in individuals of a single population. The initial rearing of different members of a family (representing similar genotypes) across different temperatures identified significant genetic variation for plasticity in a lab population of *B. anynana* (Windig 1994). In particular, variation in how each family responded to the same range of environments (temperatures) was captured via the presence of reaction norms with distinct slopes. However, further investigation concluded that this variation translated to minor changes to slopes when artificial selection was directly applied to the slope. These artificial selection experiments were of two types. The first type of experiment selected for steeper slopes by applying truncation selection for large eyespots at high temperature followed by

truncation selection on small eyespots at low temperature, in the following generation (trying to increase the slope) (Wijngaarden and Brakefield 2001). Alternatively, truncation selection was applied for small eyespots at high temperature and large eyespots at low temperature in the following generation (trying to decrease the slope) (Wijngaarden and Brakefield 2001). The second type of experiment split many individual families into four different rearing temperatures, examined what the reaction norms for each family across the three highest temperatures looked like, and then selected those families that had either the steeper or the shallower slopes by breeding from their siblings that were developing at the slowest (and lowest) temperature (Wijngaarden et al. 2002). Both types of experiment indicated that there was little to no genetic variation for slope of the reaction norms.

A different type of experiment, where artificial selection was applied to the size of the eyespots at a constant temperature (28 °C), followed by a subsequent examination of how these populations diverged in eyespot size across a range of rearing temperatures showed, again, no effects on slope of the reaction norms. All eyespots, regardless of starting size, became smaller with decreasing rearing temperature (Holloway and Brakefield 1995).

Despite the microevolutionary experiments above indicating little to no available genetic variation for selection on plasticity in a single lab population of *B. anynana*, the reality is that plasticity did evolve in this species, and this called for a broader exploration regarding the presence of plasticity in different populations of *B. anynana* and different species of *Bicyclus*.

5.4   Plasticity Across Populations and Species

Field collections have concluded that different environmental cues must be used to regulate eyespot size plasticity in different species of *Bicyclus* across Africa. When eyespot measurements of field-collected specimens were correlated with records of environmental variables, it was clear that species from southern regions, where temperature and humidity are positively correlated (warm wet season, cool dry season), use temperature as a cue to regulate eyespot size plasticity, but species from northern regions, where temperature and humidity are negatively correlated (warm dry season, cool wet season), are likely using humidity as the environmental cue that regulates eyespot size plasticity (Roskam and Brakefield 1999).

These predictions were confirmed when five species of *Bicyclus* from Southern Africa (from savannah and savannah-rainforest ecotones) and two from Equatorial Africa (rainforest) were reared in the lab under a common range of temperatures. All the species responded to temperature in a broadly similar way – ventral "exposed" eyespots became larger with increasing rearing temperature (Roskam and Brakefield 1996; Oostra et al. 2014). However, the savannah-rainforest species had steeper reaction norms relative to savannah or seasonal rainforest species (Roskam and Brakefield 1996).

Similar results were obtained in lab experiments where two southern populations of *B. anynana* (although from geographically distant locations in Malawi and South Africa) both developed larger ventral eyespots when reared at warmer temperatures, despite having diverged in absolute eyespot size at each of the temperatures (de Jong et al. 2010).

While common garden rearing experiments have yet to be performed with northern African population/species of *Bicyclus* butterflies, the general consensus emerging is that phenotypic plasticity for eyespot size, where exposed eyespots increase in size with increasing temperature, is an ancestral property for the genus *Bicyclus*, as well as for other related sayrine genera (Roskam and Brakefield 1996; Brakefield and Frankino 2009). When species move to equatorial regions where there is almost no fluctuation in temperature across the year, they do not lose their plastic response, presumably because there are few costs associated with maintaining the genetic mechanisms of temperature sensitivity in wing patterns (Oostra et al. 2014).

Broader explorations of eyespot plasticity are now necessary, beyond the satyrids, for a more complete understanding of the evolution of eyespot size plasticity. Preliminary data (S. Bhardwaj, unpublished) indicates that many nymphalid butterflies outside the satyrids show the exact opposite pattern of plasticity in eyespot size in relation to rearing temperature. High rearing temperatures lead to smaller eyespots, instead of larger eyespots. The ecological significance of these patterns as well as their underlying physiological mechanisms needs to be examined in detail in the future for a more comprehensive examination of how plasticity in eyespots evolved.

5.5 Conclusions

The ecological significance of wing pattern plasticity in *Bicyclus anynana* is becoming increasingly well understood. In particular, exposed eyespots serve a cryptic function in the dry season, whereas they serve a deflection function in the wet season. Nonexposed eyespots serve a sexual signaling function and display their own patterns of plasticity, distinct from those of exposed eyespots. In addition, patterns of plasticity for each eyespot and for each of the color components within an eyespot are very eyespot-specific and need to be studied in isolation. The physiological basis of eyespot size plasticity in this species, unfortunately, focused for a very long time on a developmental period of low temperature sensitivity (the early pupal stage) instead of the more highly sensitive wandering larval stage of development. So, much of the early work in this system needs to be read and interpreted with caution. More recent experiments have clarified the developmental window and the physiological basis for size plasticity of both dorsal and ventral eyespots, and we have only begun to explore how different homologous wing pattern elements respond to the same environmental cue in different ways. Still, much work still remains to be done. For instance, as pointed out above, different

species living in different environments are likely to use different cues to regulate homologous wing pattern elements. However, we still don't know which cues are used (besides temperature) and how they affect wing pattern development. We still don't understand how temperature regulates hormone titers in *B. anynana* and how 20E signaling regulates eyespot size, and we have no idea of the role of epigenetic processes, if any, on the regulation of this process. Finally, comparative work across species is necessary to understand when 20E hormone titers became regulated by rearing temperature at the wandering stage of development, when the ecdysone receptor became recruited to eyespot centers, making them sensitive to fluctuating 20E titers, and when genes from the eyespot gene regulatory network became sensitive to 20E signaling.

References

Bear A, Monteiro A (2013) Male courtship rate plasticity in the butterfly Bicyclus anynana is controlled by temperature experienced during the pupal and adult stages. PLoS One 8(5): e64061. doi:10.1371/journal.pone.0064061. PubMed PMID: WOS:000320362700095

Beldade P, Mateus ARA, Keller RA (2011) Evolution and molecular mechanisms of adaptive developmental plasticity. Mol Ecol 20(7):1347–1363. doi:10.1111/j.1365-294X.2011.05016.x. PubMed PMID: WOS:000288705300006

Bhardwaj S, Prudic KL, Bear A, Das Gupta M, Cheong WF, Wenk MR, et al. (2017) Sex differences in 20-hydroxyecdysone hormone levels control sexual dimorphism in butterfly wing patterns. bioRxiv, 124834.

Bradshaw AD (1956) Evolutionary significance of phenotypic plasticity in plants. In: Caspari EW (ed) Adv Genet. 13. Academic, New York, pp 115–155

Brakefield PM, Frankino WA (2009) Polyphenisms in Lepidoptera: multidisciplinary approaches to studies of evolution and development. In: Whitman DW, Ananthakrishnan TN (eds) Phenotypic plasticity in insects mechanisms and consequences. Science Publishers, Plymouth, pp 281–312

Brakefield PM, Larsen TB (1984) The evolutionary significance of dry and wet season forms in some tropical butterflies. Biol J Linn Soc 22:1–12

Brakefield PM, Mazzotta V (1995) Matching field and laboratory environments – effects of neglecting daily temperature-variation on insect reaction norms. J Evol Biol 8(5):559–573. doi:10.1046/j.1420-9101.1995.8050559.x. PubMed PMID: WOS:A1995RY61500002

Brakefield PM, Reitsma N (1991) Phenotypic plasticity, seasonal climate and the population biology of Bicyclus butterflies (Satyridae) in Malawi. Ecol Entomol 16:291–303. doi:10.1111/j.1365-2311.1991.tb00220.x

Brakefield P, Gates J, Keys D, Kesbeke F, Wijngaarden P, Monteiro A et al (1996) Development, plasticity and evolution of butterfly eyespot patterns. Nature 384(6606):236–242. doi:10.1038/384236a0. PubMed PMID: WOS:A1996VU38100042

Brakefield PM, Kesbeke F, Koch PB (1998) The regulation of phenotypic plasticity of eyespots in the butterfly *Bicyclus anynana*. Am Nat 152:853–860

Brunetti C, Selegue J, Monteiro A, French V, Brakefield P, Carroll S (2001a) The generation and diversification of butterfly eyespot color patterns. Curr Biol 11(20):1578–1585. doi:10.1016/S0960-9822(01)00502-4. PubMed PMID: WOS:000171651700015

Brunetti CR, Selegue JE, Monteiro A, French V, Brakefield PM, Carroll SB (2001b) The generation and diversification of butterfly eyespot color patterns. Curr Biol 11:1578–1585

Condamin M (1973) Monographie du genre *Bicyclus* (Lepidoptera, Satyridae). IFAN, Dakar

Costanzo K, Monteiro A (2007) The use of chemical and visual cues in female choice in the butterfly Bicyclus anynana. Proc R Soc Lond B Bio 274(1611):845–851. doi:10.1098/rspb.2006.3729. PubMed PMID: WOS:000243842100012

de Jong G (2005) Evolution of phenotypic plasticity: patterns of plasticity and the emergence of ecotypes. New Phytol 166(1):101–117. doi:10.1111/j.1469-8137.2005.01322.x. PubMed PMID: WOS:000227390500011

de Jong MA, Kesbeke F, Brakefield PM, Zwaan BJ (2010) Geographic variation in thermal plasticity of life history and wing pattern in Bicyclus anynana. Clim Res 43(1–2):91–102. doi:10.3354/cr00881. PubMed PMID: WOS:000280830000010

Dinan L, Whiting P, Girault JP, Lafont R, Dhadialla TS, Cress DE et al (1997) Cucurbitacins are insect steroid hormone antagonists acting at the ecdysteroid receptor. Biochem J 327:643–650. PubMed PMID: ISI:A1997YF86500003

Dion E, Monteiro A, Yew JY (2016) Phenotypic plasticity in sex pheromone production in *Bicyclus anynana* butterflies. Sci Report 6:39002. doi:10.1038/srep39002

Everett A, Tong XL, Briscoe AD, Monteiro A (2012) Phenotypic plasticity in opsin expression in a butterfly compound eye complements sex role reversal. BMC Evol Biol 12:232. doi:10.1186/1471-2148-12-232. PubMed PMID: WOS:000313877800001

Fischer K, Brakefield PM, Zwaan BJ (2003a) Plasticity in butterfly egg size: why larger offspring at lower temperatures? Ecology 84(12):3138–3147. doi:10.1890/02-0733

Fischer K, Eenhoorn E, Bot AN, Brakefield PM, Zwaan BJ (2003b) Cooler butterflies lay larger eggs: developmental plasticity versus acclimation. Proc R Soc B 270(1528):2051–2056. PubMed PMID: 14561294

French V, Brakefield PM (1992) The development of eyespot patterns on butterfly wings: morphogen sources or sinks? Development 116:103–109

Ho S, Schachat SR, Piel WH, Monteiro A (2016) Attack risk for butterflies changes with eyespot number and size. R Soc Open Sci 3:150614

Holloway GJ, Brakefield PM (1995) Artificial selection of reaction norms of wing pattern elements in Bicyclus-anynana. Heredity 74:91–99. PubMed PMID: ISI:A1995QA25300011

Koch PB, Buckmann D (1987) Hormonal-control of seasonal morphs by the timing of ecdysteroid release in Araschnia levana L (Nymphalidae, Lepidoptera). J Insect Physiol 33(11):823–829. PubMed PMID: ISI:A1987K176700006

Koch PB, Brakefield PM, Kesbeke F (1996) Ecdysteroids control eyespot size and wing color pattern in the polyphenic butterfly *Bicyclus anynana* (Lepidoptera, Satyridae). J Insect Physiol 42:223–230

Kooi RE (1995) The effect of food plant quality on wing pattern induction in the tropical butterfly Bicyclus anynana (Satyrinae). In: Sommeijer MJ, Francke PJ (eds), pp 107–112

Kooi RE, Brakefield PM. The critical period for wing pattern induction in the polyphenic tropical butterfly Bicyclus anynana (Satyrinae). J Insect Physiol 1999;45(3):201–212. PubMed

Lyytinen A, Brakefield PM, Mappes J (2003) Significance of butterfly eyespots as an anti-predator device in ground-based and aerial attacks. Oikos 100(2):373–379. PubMed PMID: ISI:000181854900018

Lyytinen A, Brakefield PM, Lindstrom L, Mappes J (2004) Does predation maintain eyespot plasticity in *Bicyclus anynana*? Proc R Soc Lond B Bio 271(1536):279–283. PubMed PMID: ISI:000188694400010

Macias-Munoz A, Smith G, Monteiro A, Briscoe AD (2016) Transcriptome-wide differential gene expression in Bicyclus anynana butterflies: female vision-related genes are more plastic. Mol

Biol   Evol   33(1):79–92.   doi:10.1093/molbev/msv197.   PubMed   PMID:
    WOS:000369992600006

Mateus ARA, Marques-Pita M, Oostra V, Lafuente E, Brakefield PM, Zwaan BJ et al (2014)
    Adaptive developmental plasticity: compartmentalized responses to environmental cues and to
    corresponding internal signals provide phenotypic flexibility. BMC Biol 12:97. doi:10.1186/
    s12915-014-0097-x. PubMed PMID: WOS:000348150100001

Monteiro A, Brakefield P (1994) French v. The evolutionary genetics and developmental basis of
    wing pattern variation in the butterfly bicyclus-anynana. Evol Int J Org Evol 48(4):1147–1157.
    doi:10.2307/2410374. PubMed PMID: WOS:A1994QE32300018

Monteiro A, Glaser G, Stockslager S, Glansdorp N, Ramos D (2006) Comparative insights into
    questions of lepidopteran wing pattern homology. BMC Dev Biol 6. doi:10.1186/1471-213X-
    6-52. PubMed PMID: WOS:000242189200001

Monteiro A, Tong XL, Bear A, Liew SF, Bhardwaj S, Wasik BR et al (2015) Differential
    expression of ecdysone receptor leads to variation in phenotypic plasticity across serial
    homologs.   PLoS   Genet   11(9).   doi:10.1371/journal.pgen.1005529.   PubMed   PMID:
    WOS:000362269000043

Moran NA (1992) The evolutionary maintenance of alternative phenotypes. Am Nat 139
    (5):971–989. PubMed PMID: ISI:A1992HU07100005

Nijhout HF (1980) Ontogeny of the color pattern on the wings of *Precis coenia* (Lepidoptera:
    Nymphalidae). Dev Biol 80:275–288

Nijhout HF (1999) Control mechanisms of polyphenic development in insects. Bioscience 49
    (3):181–192. doi:10.2307/1313508

Nijhout HF (2003) Development and evolution of adaptive polyphenisms. Evol Dev 5(1):9–18.
    doi:10.1046/j.1525-142X.2003.03003.x. PubMed PMID: WOS:000179925400003

Oliver JC, Ramos D, Prudic KL, Monteiro A (2013) Temporal gene expression variation associ-
    ated with eyespot size plasticity in Bicyclus anynana. PLoS One 8(6). doi:10.1371/journal.
    pone.0065830. PubMed PMID: WOS:000320440500052

Olofsson M, Jakobsson S, Wiklund C (2013) Bird attacks on a butterfly with marginal eyespots and
    the role of prey concealment against the background. Biol J Linn Soc 109(2):290–297. doi:10.
    1111/bij.12063. PubMed PMID: WOS:000318809500004

Oostra V, de Jong MA, Invergo BM, Kesbeke F, Wende F, Brakefield PM et al (2011) Translating
    environmental gradients into discontinuous reaction norms via hormone signalling in a
    polyphenic butterfly. Proc R Soc B Biol Sci 278(1706):789–797. doi:10.1098/rspb.2010.
    1560. PubMed PMID: ISI:000286507400021

Oostra V, Brakefield PM, Hiltemann Y, Zwaan BJ, Brattstrom O (2014) On the fate of seasonally
    plastic traits in a rainforest butterfly under relaxed selection. Ecol Evol 4(13):2654–2667.
    doi:10.1002/ece3.1114. PubMed PMID: WOS:000339494900004

Orme MH, Leevers SJ Flies on steroids: the interplay between ecdysone and insulin signaling. Cell
    Metab 2(5):277–278. doi:10.1016/j.cmet.2005.10.005

Prudic KL, Jeon C, Cao H, Monteiro A (2011) Developmental plasticity in sexual roles of butterfly
    species drives mutual sexual ornamentation. Science 331(6013):73–75. doi:10.1126/science.
    1197114. PubMed PMID: WOS:000285974000038

Prudic KL, Stoehr AM, Wasik BW, Monteiro A (2015) Invertebrate predators attack eyespots and
    promote the evolution of phenotypic plasticity. Proc R Soc Lond B Bio 282(1798):20141531

Robertson K, Monteiro A (2005) Female Bicyclus anynana butterflies choose males on the basis of
    their dorsal UV-reflective eyespot pupils. Proc R Soc Lond B Bio 272(1572):1541–1546.
    doi:10.1098/rspb.2005.3142. PubMed PMID: WOS:000231504300003

Roskam JC, Brakefield PM (1996) A comparison of temperature-induced polyphenism in African
    Bicyclus butterflies from a savannah-rainforest ecotone. Evol Int J Org Evol 50:2360–2372

Roskam JC, Brakefield PM (1999) Seasonal polyphenism in Bicyclus (Lepidoptera: Satyridae)
    butterflies: different climates need different cues. Biol J Linn Soc 66(3):345–356. doi:10.1111/
    j.1095-8312.1999.tb01895.x. PubMed PMID: WOS:000079376200005

Rountree DB, Nijhout HF (1995) Hormonal control of a seasonal polyphenism in precis coenia (Lepidoptera: Nymphalidae). J Insect Physiol 41(11):987–992

Stearns SC (1989) The evolutionary significance of phenotypic plasticity. Bioscience 39 (7):436–445. PubMed PMID: ISI:A1989AC84800005

Vlieger L, Brakefield PM (2007) The deflection hypothesis: eyespots on the margins of butterfly wings do not influence predation by lizards. Biol J Linn Soc 92(4):661–667. PubMed PMID: WOS:000251414500006

West-Eberhard MJ (2003) Developmental plasticity and evolution. Oxford University Press, New York, 794 p

Westerman E, Monteiro A (2016) Rearing temperature influences adult response to changes in mating status. PLoS One 11(2):e0146546. doi:10.1371/journal.pone.0146546. PubMed PMID: WOS:000370046600012

Wijngaarden PJ, Brakefield PM (2001) Lack of response to artificial selection on the slope of reaction norms for seasonal polyphenism in the butterfly Bicyclus anynana. Heredity 87:410–420. doi:10.1046/j.1365-2540.2001.00933.x. PubMed PMID: WOS:000172693900004

Wijngaarden PJ, Koch PB, Brakefield PM (2002) Artificial selection on the shape of reaction norms for eyespot size in the butterfly Bicyclus anynana: direct and correlated responses. J Evol Biol 15(2):290–300. doi:10.1046/j.1420-9101.2002.00380.x. PubMed PMID: WOS:000174709000012

Windig JJ (1994) Reaction norms and the genetic-basis of phenotypic plasticity in the wing pattern of the butterfly Bicyclus anynana. J Evol Biol 7(6):665–695. doi:10.1046/j.1420-9101.1994.7060665.x. PubMed PMID: ISI:A1994PV78800002

Windig JJ, Brakefield PM, Reitsma N, Wilson JGM (1994) Seasonal polyphenism in the wild: survey of wing patterns in five species of *Bicyclus* butterflies in Malawi. Ecol Entomol 19:285–298

Zera AJ (2007) Endocrine analysis in evolutionary-developmental studies of insect polymorphism: hormone manipulation versus direct measurement of hormonal regulators. Evol Dev 9 (5):499–513. PubMed PMID: ISI:000249321200009

Chapter 6
Spatial Variation in Boundary Conditions Can Govern Selection and Location of Eyespots in Butterfly Wings

Toshio Sekimura and Chandrasekhar Venkataraman

Abstract Despite being the subject of widespread study, many aspects of the development of eyespot patterns in butterfly wings remain poorly understood. In this work, we examine, through numerical simulations, a mathematical model for eyespot focus point formation in which a reaction-diffusion system is assumed to play the role of the patterning mechanism. In the model, changes in the boundary conditions at the veins at the proximal boundary alone are capable of determining whether or not an eyespot focus forms in a given wing cell and the eventual position of focus points within the wing cell. Furthermore, an auxiliary surface reaction-diffusion system posed along the entire proximal boundary of the wing cells is proposed as the mechanism that generates the necessary changes in the proximal boundary profiles. In order to illustrate the robustness of the model, we perform simulations on a curved wing geometry that is somewhat closer to a biological realistic domain than the rectangular wing cells previously considered, and we also illustrate the ability of the model to reproduce experimental results on artificial selection of eyespots.

Keywords Butterfly patterning • Eyespot pattern • Focus point formation • Turing patterns • Reaction-diffusion system • Surface reaction-diffusion system • Surface finite element method

T. Sekimura
Department of Biological Chemistry, Graduate School of Bioscience and Biotechnology, Chubu University, Kasugai, Aichi 487-8501, Japan
e-mail: sekimura@isc.chubu.ac.jp

C. Venkataraman (✉)
School of Mathematics and Statistics, University of St Andrews, Fife KY16 9SS, UK
e-mail: cv28@st-andrews.ac.uk

6.1   Introduction

Eyespots, concentric bands of pigment patterning, constitute one of the most studied pattern elements on the wings of butterflies (c.f., Fig. 6.3 for an example). Each eyespot develops around a focus, a small group of cells that sends out a morphogenetic signal that determines the synthesis of circular patterns of pigments in their surroundings. In this work, we consider a model that provides a possible mechanism underlying the determination of the number and locations of eyespots on the wing surface. The model we consider, first described by Sekimura et al. (2015), provides a mechanism that places the foci around which eyespots form in various locations on the entire wing surface. We do not address here subsequent stages of eyespot formation that occurs after the development of the foci.

The model we consider is based on that of Nijhout (1990). The main novelty of the work in Sekimura et al. (2015) was to illustrate that simply changing the conditions assumed to hold at the proximal veins was sufficient to determine whether or not an eyespot formed in a given wing cell. In the present work, we extend the investigations of the models proposed in Sekimura et al. (2015). We show that it is possible to determine the location of eyespots within a wing cell simply by changing the conditions that are assumed to hold at the lateral wing veins that bound the wing cell. Furthermore, we illustrate that it is possible, using a two-stage model, to recapitulate the results of artificial selection experiments in terms of selection and location of eyespots in butterfly wings.

6.2   Modelling

In this section, we describe the mathematical model for focus point formation that we consider in the present work.

6.2.1   Setting

As butterfly wing patterns form in two layers that are thought to be separated completely by the middle tissue (e.g. Sekimura et al. 1998), we assume that the formation of eyespots takes place in a single layer of the wing disc. Hence, we model the domain in which eyespot formation occurs as a two-dimensional region. Furthermore, we assume that this two-dimensional region consists of several wing cells, regions bounded by the wing veins, and we consider a region of up to seven wing cells sufficient to represent the entire surface (front or back) of the wing disc. For the sake of simplicity, we assume that each of the wing cells is of the same shape and size.

The model we consider for the formation of focus points is based on that proposed by Nijhout (1990) and consists of a reaction-diffusion system of activator-inhibitor type (Gierer and Meinhardt 1972) posed in each wing cell with time-independent Dirichlet boundary conditions (i.e. a source of chemicals) on the wing veins and Neumann (zero flux) boundary conditions (i.e. no flux of chemicals) at the wing margin.

6.2.2   Mathematical Model

We denote by n_{seg} the number of wing cells. We denote by Ω_i the ith wing cell with boundaries $\Gamma_{m,i}$ (wing margin), $\Gamma_{v,i}, \Gamma_{v,i+1}$ (veins) and $\Gamma_{p,i}$ (proximal boundary). The boundary conditions for the activator (a_1) are Dirichlet (fixed) on the proximal boundary $\Gamma_{p,i}$ and the wing veins $\Gamma_{v,i}, \Gamma_{v,i+1}$ and Neumann (zero flux) on the wing margin $\Gamma_{m,i}$ (c.f., Fig. 6.1). The boundary conditions for the inhibitor (a_2) are zero
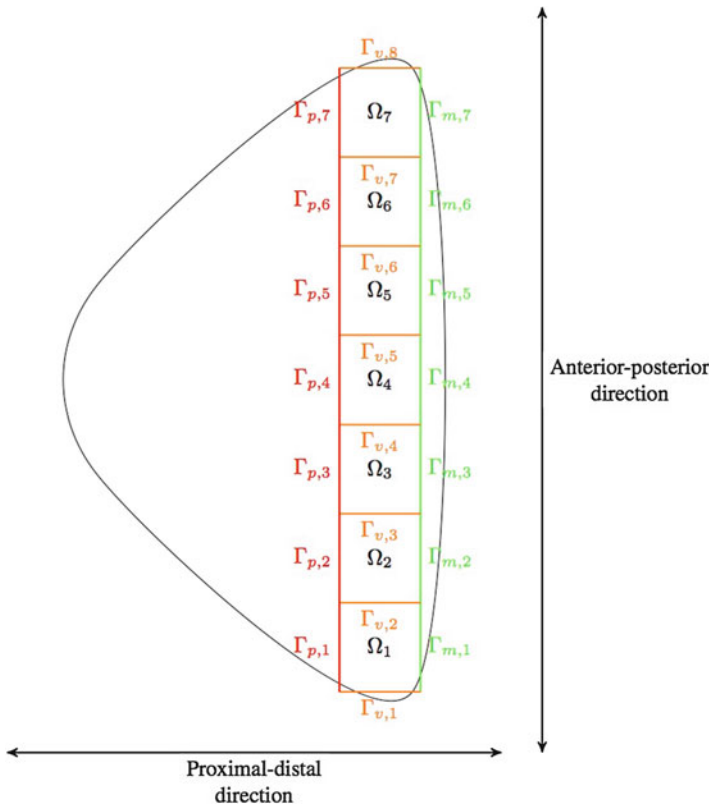
Fig. 6.1 A sketch of the domain on which we model the formation of eyespot focus points

flux on all four boundaries of each wing cell. The Dirichlet boundary condition on each vein $\Gamma_{v,i}$ is the same for each vein. We take the initial data for both activator and inhibitor to be the positive spatially homogeneous steady state of the Gierer-Meinhardt (GM) equation. Thus, our model for focus pattern formation consists of n_{seg}-independent GM equations. The model system equations may be stated as follows:

For $i = 1, \ldots, n_{\text{seg}}$, find $\vec{a}(\vec{x}, t)$, $(\vec{x}, t) \in \Omega \times (0, T)$, such that

$$
\begin{aligned}
\partial_t \vec{a}(\vec{x}, t) - D\Delta \vec{a}(\vec{x}, t) = \vec{f}(\vec{a}(\vec{x}, t)) \quad & (\vec{x}, t) \in \Omega_i \times (0, T) \\
a_1(\vec{x}, t) = u(\vec{x}) \quad & \vec{x} \in \partial \Omega_i / \Gamma_{m,i} \\
\nabla a_1(\vec{x}, t) \cdot \vec{n}(\vec{x}, t) = 0 \quad & (\vec{x}, t) \in \Gamma_{m,i} \times (0, T) \\
\nabla a_2(\vec{x}, t) \cdot \vec{n}(\vec{x}, t) = 0 \quad & (\vec{x}, t) \in \partial \Omega_i \times (0, T) \\
\vec{a}(\vec{x}, t) = \vec{a}^{ss} \quad & \vec{x} \in \Omega_i,
\end{aligned}
\tag{6.1}
$$

where D is a diagonal matrix of positive diffusion coefficients and the reaction kinetic vector $\vec{f}(\vec{v})$ is given by $f_1(\vec{v}) = \alpha\big((\kappa_1 v_1^2 / v_2) - \kappa_2 v_1\big)$ and $f_2(\vec{v}) = \alpha\big(\kappa_1 v_1^2 - \kappa_3 v_2\big)$, with $\kappa_1, \kappa_2, \kappa_3 > 0$. The choice of kinetics yields that the corresponding ODE system has a positive steady $\vec{a}^{ss} = (\kappa_2/\kappa_2, \kappa_1 \kappa_3/\kappa_2)^T$.

Nijhout (1990, 1994) showed that the above model was capable of generating source profiles consistent with the formation of an eyespot focus within a wing cell. In Sekimura et al. (2015), we showed that changes in the Dirichlet boundary condition for a_1 at the proximal boundary $\Gamma_{p,i}$ alone were sufficient to determine whether or not an eyespot focus forms in a wing cell. For the proximal boundary profile, we consider two different cases firstly, prescribed boundary conditions, and secondly, in order to propose a full model, we consider that the boundary profiles are themselves generated by a patterning mechanism that is posed along the entire proximal boundary, i.e. the *curved surface* $\Gamma_p := \cup_i \Gamma_{p,i}$. For this one-dimensional patterning mechanism, for consistency with the two-dimensional model above, we consider a surface reaction-diffusion system which for illustrative purposes we choose to be the activator-depleted substrate model of Schnakenberg (1979), stated as follows:

Find $\vec{u}(\vec{x}, t)$ such that

$$
\partial_t \vec{u}(\vec{x}, t) - D_u \Delta_\Gamma \vec{u}(\vec{x}, t) = \vec{h}(\vec{u}(\vec{x}, t)) \quad \text{on } \Gamma_p,
\tag{6.2}
$$

where D_u is a diagonal matrix of positive diffusion coefficients, Δ_Γ is the Laplace-Beltrami operator (the analogue to the usual Cartesian Laplacian on the surface) and the function $\vec{h}(\vec{u})$ is given by $h_1(\vec{u}) = \gamma(\vec{x})\big(a - u_1 + u_1^2 u_2\big)$ and $h_2(\vec{u}) = \gamma(\vec{x}) \big(b - u_1^2 u_2\big)$, with $a, b > 0$. u_1 and u_2 are the concentrations of two chemicals (the activator and substrate, respectively). The function γ can be thought of as a reaction rate and is typically taken to be constant in most studies that employ such systems to model biological pattern formation. However, if such an approach is adopted, patterns with a constant wavelength across Γ_p are to be expected. In the present

context, this would be insufficient to explain butterfly wing patterning in which the distribution of eyespots occurs with differing frequency in different parts of the wing. For this reason, we allow the reaction rate to be a function of space, which appears to provide sufficient freedom to generate the necessary source profiles from this one-dimensional model that produces any arbitrary eyespot configuration observed on butterfly wings. The resulting model is a *two-stage* model for focus point formation in which the first stage corresponds to solving the Schnakenberg surface reaction-diffusion system Eq. (6.2) to steady state and in the second stage the solution u_2 to this model is used to determine the proximal boundary profiles for a_1 in the eyespot reaction-diffusion system model Eq. (6.1) within each of the wing cells.

6.3   Computational Approximation

For the approximation of the eyespot reaction-diffusion system models posed within each of the wing cells, we employ an implicit-explicit finite element method developed and analysed in Lakkis et al. (2013). An advantage of such an approach is that arbitrary, potentially evolving, geometries can be considered. In particular, one does not need to assume that the wing cells are rectangular, and indeed using open-source meshing software, it is even possible to solve the systems on geometries obtained from image data, which may be a worthwhile extension. For the approximation of the surface reaction-diffusion system, we employ the surface finite element method (Dziuk and Elliott 2013). We refer to the above two references for further details on the numerical approach.

6.4   Results

6.4.1   Gradients in Source Strength on the Wing Veins Can Determine Eyespot Location in the Wing Cell

We start by illustrating that in the eyespot focus point formation model of Sect. 6.2, it is possible to change the location of eyespots by allowing the Dirichlet boundary condition at the wing veins to vary in space. To this end, we suppose that the wing cells are trapezoidal with parallel sides corresponding to the proximal and marginal boundaries that are chosen to be of length 1.5 and 2.5, respectively and are such that the height (proximal-marginal) is 3. We set the proximal boundary condition to be a convex profile of the form $u(\vec{x}) = 2a_1^{ss}(1 - \sin^2(\pi d(\vec{x})/1.5))$ where $d(\vec{x})$ is the distance from the boundary points of the proximal boundary. The boundary

Table 6.1 Parameter values for simulations of Sect. 6.4.1

D_1	D_2	α	κ_1	κ_2	κ_3
0.0031	0.03	20	0.03	0.03	0.0125

condition thus takes the value $2a_1^{ss}$ at the boundary points of $\Gamma_{p,i}$ and decays to 0 at the centre of the proximal boundary. For the wing veins, we consider a gradient in the Dirichlet boundary condition by considering a linear boundary condition of the form $u(\vec{x}) = 2a_1^{ss}(1 - s_1 x_2/3)$, where x_2 denotes the distance in the proximal-distal direction from the wing margin and $s_1 > 0$ is a parameter that governs the magnitude of the gradient. Thus the boundary condition takes the value $2a_1^{ss}$ at the point where the vein meets the marginal boundary and decays towards the proximal boundary with slope given by $s_1 > 0$. The remaining parameter values we select are given in Table 6.1. For the discretisation we used linear finite elements on a grid with 2145 degrees of freedom (DOFs) and a time step of 0.01. The system was solved until the discrete solution was (approximately) at steady state.

Figure 6.2a–d shows snapshots of the activator a_1 concentration at different times for different values of s_1. In each of the subfigures, the value of $s_1 = 0, 0.15, 0.25, 0.35, 0.45, 0.5$ reading from left to right. We see that in the case of constant boundary conditions or if the gradient is small ($s_1 = 0, 0.15, 0.25, 0.35$), the centreline peak, characteristic of the Nijhout model, does not extend very far from the margin. The focus point forms near the middle of the wing cell and migrates towards the wing margin with the steady state corresponding to a single focus near the margin. For larger values of the gradient ($s_1 = 0.45, 0.5$), the centreline peak extends much further, almost reaching the proximal boundary, and the resulting focus point forms close to the proximal boundary. The focus point migrates downwards only until around the centre of the wing cell, and the resulting steady state is a single focus point around the centre of the wing cell.

6.4.2 A Surface Reaction-Diffusion System Model with Piecewise Constant Reaction Rate Generates Boundary Profiles and Resulting Eyespot Foci Recapitulate Those Observed in Artificial Selection

We now report on simulations in which we illustrate that the two-stage model proposed in Sect. 6.2 (see also, Sekimura et al. 2015) is capable of reproducing the differing selection of dorsal forewing eyespots observed in artificial selection experiments on *Bicyclus anynana*. Beldade et al. (2002) showed that, through artificial selection, it is possible to generate different phenotypes of *B. anynana* with either zero, one (anterior or posterior) or two forewing eyespots (anterior and posterior) (c.f., Fig. 6.3). To investigate whether our two-stage model is capable of
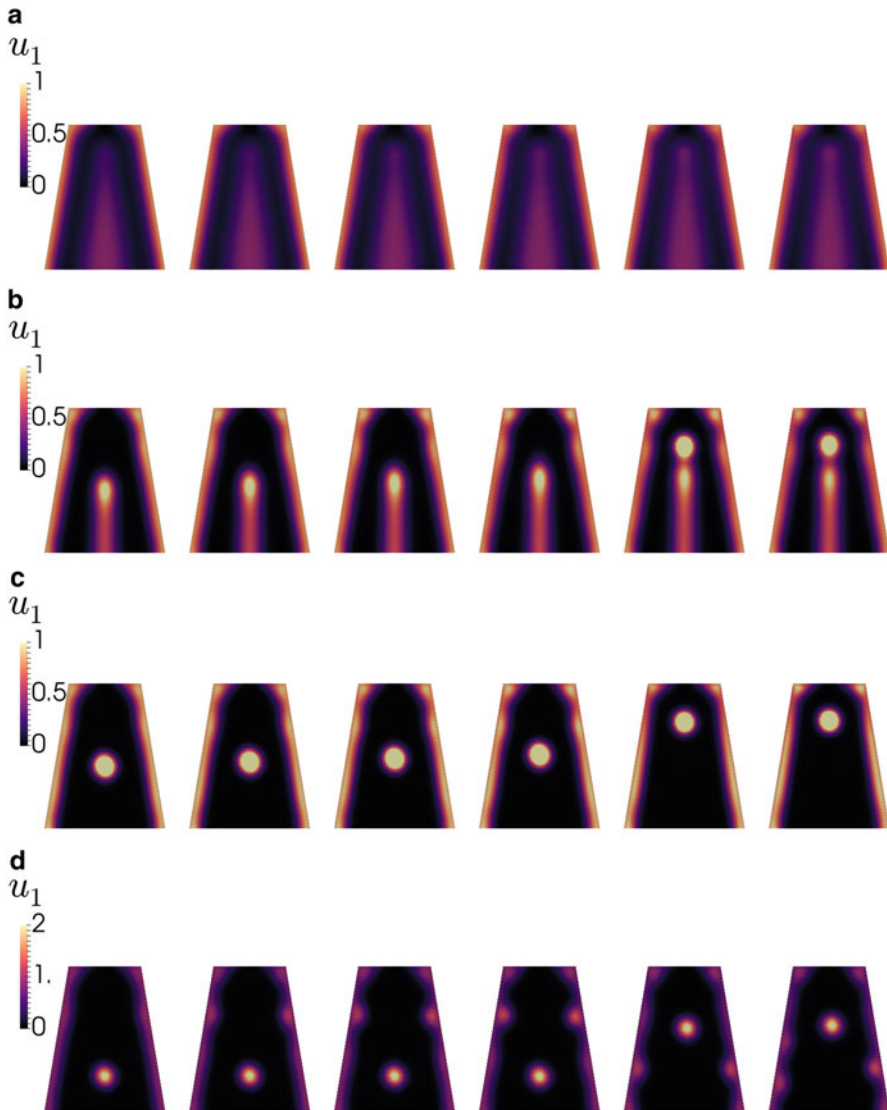
Fig. 6.2 Eyespot focus point formation on a trapezoidal domain. On the wing veins we take a Dirichlet boundary condition of the form $u(\vec{x}) = 2a_1^{ss}(1 - s_1 x_2/3)$. In each of the subfigures, the gradient in the Dirichlet boundary condition is increasing with $s_1 = 0, 0.15, 0.25, 0.35, 0.45, 0.5$ reading from *left* to *right*. Thus the leftmost snapshot in each subfigure corresponds to constant Dirichlet boundary conditions on the wing veins, whilst the rightmost snapshot in each subfigure corresponds to the steepest linear gradient with $u(\vec{x}) = 2a_1^{ss}$ at the point where the wing veins meet the margin and $u(\vec{x}) = a_1^{ss}$ at the point where the wing veins meet the proximal boundary. In all the subfigures, we only display snapshots of the activator a_1 concentration; the inhibitor concentrations are in phase with those of the activator and are thus omitted. For remaining parameter values, see text. (**a**) $t=0.1$. (**b**) $t=0.2$. (**c**) $t=0.5$. (**d**) Steady state

Fig. 6.3 Eyespot
phenotypes of *B. anynana*
produced in artificial
selection experiments
(Beldade et al. 2002)
(Figure reproduced with
permission of the publisher)
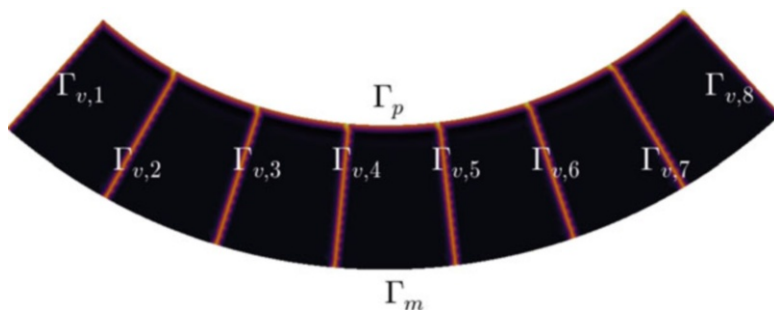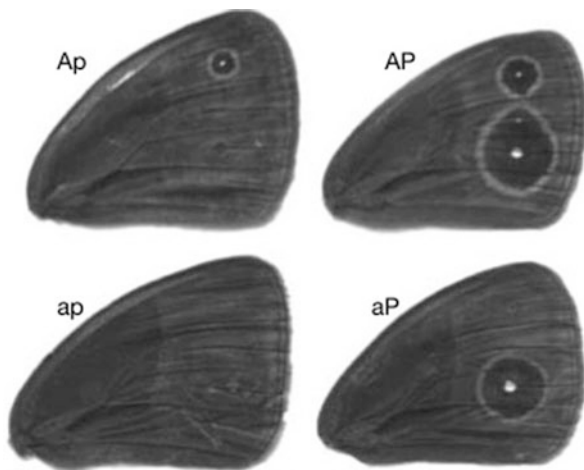
Fig. 6.4 Sketch of the geometry used to model the entire region of the wing disc on which eyespot
formation occurs for the experiments of Sect. 6.4.2

reproducing these observations, we consider a wing as shown in Fig. 6.4. The
proximal (Γ_p) and marginal (Γ_m) boundaries are curves corresponding to a portion
of the circumference of two concentric circles of radius 9 and 12, respectively. The
wing veins ($\Gamma_{v,i}$) are assumed to be radial and of length 3, whilst the proximal and
marginal boundaries of each of the wing cells are approximately of length 1.88 and
3.35, respectively. We consider the two-stage model described in Sect. 6.2. In the
first stage, we solve the surface reaction-diffusion system with the Schnakenberg
kinetics to steady state. We select Dirichlet (prescribed) boundary conditions for u_1
with $u_1 = u_1{}^{ss}$ on one boundary and $u_1 = 2u_1{}^{ss}$ at the other boundary point. For u_2 we
set zero-flux boundary conditions. The initial data is taken to be the steady state
value for both u_1 and u_2. We consider the case that the function γ is piecewise

Table 6.2 Parameter values for simulations of Sect. 6.4.2

D_{u1}	D_{u2}	a	b	D_1	D_2	α	κ_1	κ_2	κ_3
1	15	0.1	0.9	0.005	0.03	20	0.03	0.03	0.0125

constant (e.g. McMillan et al. 2002); in particular, we allow it to take two distinct values on either side of the midpoint (anterior-posterior) of the proximal boundary curve. The remaining parameter values we employed are shown in Table 6.2. After solving the Schnakenberg system to steady state, we assume the Dirichlet boundary condition at the proximal boundary for the reaction-diffusion system posed in each wing cell is of the form

$$a_1(\vec{x}, t) = 1.9\bar{u}_2(\vec{x})a_1^{SS} \vec{x} \in \Gamma_{p,i},$$

where $\bar{u}_2(\vec{x})$ is the spatially inhomogeneous steady state of the substrate in the Schnakenberg equation. At the veins, we set Dirichlet boundary conditions for the activator equal to twice the steady state value. The remaining parameter values are given in Table 6.2. We note that each wing cell in this simulation is slightly larger in area than those considered in Sect. 6.4.1, and it is due to this fact that we require a slightly larger activator diffusivity, D_1, than that which was used in Sect. 6.4.1.

For the numerical parameters, we used a mesh with 3927 DOFs to represent the entire wing disc. The surface reaction-diffusion system was solved on the trace mesh corresponding to the boundary edges of the bulk mesh; the corresponding one-dimensional mesh had 1793 DOFs. We used a piecewise linear finite element method for both the surface and bulk reaction-diffusion systems with a time step of 0.05, and we solved the system until the concentration profiles were (approximately) at steady state. Figure 6.5 shows the steady state values obtained for simulations in which we vary the value of the piecewise constant reaction rate γ. We see that when γ is zero in both the anterior and posterior, as expected the substrate concentration (that satisfies zero-flux boundary conditions) in the one-dimensional system simply converges to a constant. Using this profile in the proximal boundary conditions for the model posed in each wing cell, we generate a wing with no foci similar to the *ap* case of Fig. 6.3. If we allow γ to be large on one half of the proximal boundary and small on the other half, then we generate boundary profiles from the one-dimensional system that results in a single eyespot in the half of the wing in which γ is large, similar to the *Ap* and *aP* phenotypes of Fig. 6.3. Finally, if γ is large and constant across the entire proximal boundary, we generate a profile that leads to both the anterior and posterior foci forming as in the *AP* phenotype of Fig. 6.3. The choice of Dirichlet boundary conditions for u_1 leads the substrate troughs to form in the correct locations for the eventual eyespots dependent on whether they are anterior or posterior; as for zero-flux or symmetric Dirichlet boundary conditions, we would expect solutions that are symmetric along the midpoint of the proximal boundary. We note that this asymmetry need not be
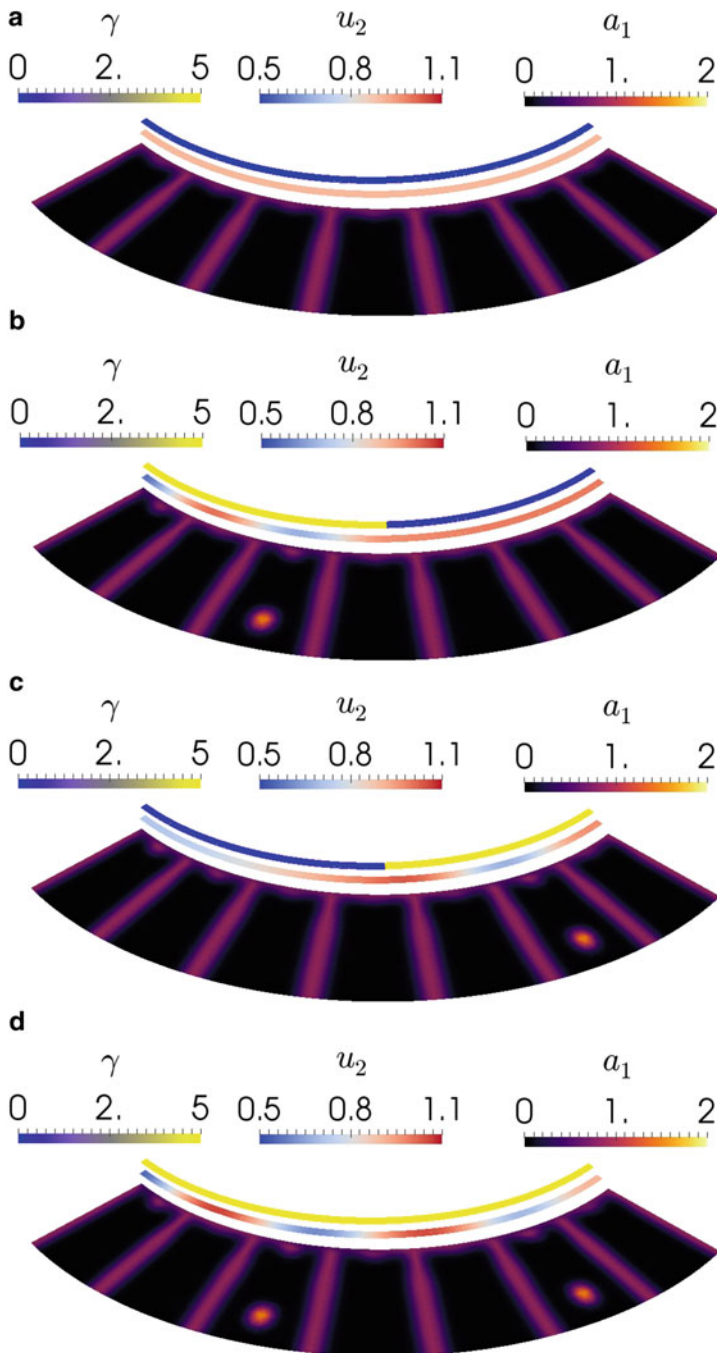
Fig. 6.5 Simulations of eyespot focus point formation using a two-stage model. Initially a reaction-diffusion system with the Schnakenberg kinetics is solved to steady state on the curved

through Dirichlet boundary conditions and could be the result of differences between individual wing cells or some other aspect which is thus far neglected in the modelling.

6.5   Discussion

In this study, we reported on further investigations of a model for the selection and distribution of eyespot foci, originally presented in the paper (Sekimura et al. 2015). The basic idea of the model is that whether an eyespot focus forms in a given wing cell and its eventual position in the wing cell can be determined through changing only the boundary conditions that are assumed to hold at the veins. Furthermore, we considered a two-stage model consisting of two related pattern-forming mechanisms, one posed along the proximal vein and the other posed in each wing cell. The two-stage model appears capable of reproducing the results of artificial selection experiments in terms of eyespot selection. A hypothesis within the two-stage model is that patterning in the first stage could be governed by a reaction-diffusion mechanism in which the reaction rate is dependent on the spatial position. Such an assumption is consistent with assuming different levels of gene activation in different regions of the wing (e.g. McMillan et al. 2002). We note however that the present model is still sensitive to changes in the parameter values and crucially, changes in the geometry. In particular, the naturally observed variations in wing cell size across butterflies appear too large for the present model to be applicable. Hence a potentially attractive avenue for future studies is to investigate Turing systems with a degree of scale invariance as has been attempted in other contexts (e.g. Othmer and Pate 1980).

Fig. 6.5 (continued) proximal boundary using a piecewise constant value for the parameter γ, Dirichlet boundary conditions for u_1 and zero-flux boundary conditions for u_2 (see text for further details). The Dirichlet boundary condition on the proximal boundary is taken to be proportional to the substrate concentration u_2 of the Schnakenberg equation. The remaining boundary conditions and parameter values are given in the text. (**a**) Steady state values of u_2 and a_1 for constant $\gamma = 0$, corresponding to no eyespot foci. (**b**) Steady state values of u_2 and a_1 for piecewise constant $\gamma = 500$ on one half of the wing and $\gamma = 10$ on the other half, corresponding to one eyespot focus on the half of the wing with increased γ. (**c**) Steady state values of u_2 and a_1 for piecewise constant $\gamma = 10$ on one half of the wing and $\gamma = 500$ on the other half, corresponding to one eyespot focus on the half of the wing with increased γ. (**d**) Steady state values of u_2 and a_1 for constant $\gamma = 500$, corresponding to two eyespot foci

References

Beldade P, Koops K, Brakefield PM (2002) Developmental constraints versus flexibility in morphological evolution. Nature, 416(6883):844–847. PMID: 11976682

Dziuk G, Elliott CM (2013) Finite element methods for surface PDEs. Acta Numerica 22:289–396

Gierer A, Meinhardt H (1972) A theory of biological pattern formation. Biol Cyber 12(1):30–39

Lakkis O, Madzvamuse A, Venkataraman C (2013) Implicit–explicit timestepping with finite element approximation of reaction–diffusion systems on evolving domains. SIAM J Num Anal 51(4):2309–2330

McMillan WO, Monteiro A, Kapan DD (2002) Development and evolution on the wing. Trends Ecol Evol 17(3):125–133

Nijhout HF (1990) A comprehensive model for colour pattern formation in butterflies. Proc R Soc Lond B 239(1294):81–113

Nijhout HF (1994) Genes on the wing. Science, 265(5168):44–45. PMID: 7912450

Othmer HG, Pate E (1980) Scale-invariance in reaction-diffusion models of spatial pattern formation. Proc Nat Acad Sci 77(7):4180–4184

Sekimura T, Maini PK, Nardi JB, Zhu M, Murray JD (1998) Pattern formation in lepidopteran wings. Comments in Theoretical Biology 5(2–4):69–87

Sekimura, T., Venkataraman, C. and Madzvamuse, A. (2015). A model for selection of eyespots on butterfly wings. PLoS ONE. http://dx.doi.org/10.1371/journal.pone.0141434

Schnakenberg J (1979). Simple chemical reaction systems with limit cycle behaviour. J Theor Biol, 81 (3):389–400. PMID: 537379

Chapter 7
Self-Similarity, Distortion Waves, and the Essence of Morphogenesis: A Generalized View of Color Pattern Formation in Butterfly Wings

Joji M. Otaki

> Anyhow, exploring the *consequences* of self-similarity was proving full of extraordinary surprises, helping me to understand the fabric of nature.—Benoit B. Mandelbrot (1983). *The Fractal Geometry of Nature*. Revised edition, Page 423

Abstract The morphology of multicellular organisms can be viewed as structures of three-dimensional bulges and dents of an otherwise nearly two-dimensional epithelial sheet. Morphogenesis is thus a process to stably form those physical distortions over time through differential cellular adhesion, contraction, and aggregation and through cellular changes in size, shape, and number. Such physical distortions may be hierarchically repeated with modifications, which is suggested by self-similar structures in organisms. Butterfly wings are nearly two-dimensional but contain three-dimensional bulges and dents that correspond to organizing centers for color pattern elements. Importantly, an eyespot and its corresponding parafocal element on a wing, constituting the border symmetry system, are self-similar. From this perspective, I review here the color pattern rules and several formal models that have been proposed, clarifying their relationships with the induction model for positional information. To reinforce the induction model, I propose the distortion hypothesis, in which dynamic epithelial distortion forces at organizing centers, such as the center of a presumptive eyespot, that are produced through changes in cell size spread to surrounding immature cells over distances as morphogenic signals in developing butterfly wings. The physical distortion forces open stretch-activated calcium channels that cause calcium signals in the cell and activate the expression of regulatory genes. These regulatory gene products initiate

J.M. Otaki (✉)
The BCPH Unit of Molecular Physiology, Department of Chemistry, Biology and Marine Science, Faculty of Science, University of the Ryukyus, Senbaru, Nishihara, Okinawa 903-0213, Japan
e-mail: otaki@sci.u-ryukyu.ac.jp

a cascade of structural genes that eventually produce eyespot black rings. Calcium waves also activate a process of genome duplication, resulting in an increase in cell size, as the ploidy hypothesis states. A new distortion of epithelial cells is induced at the center of a presumptive parafocal element through an increase in cell size, producing self-similarity of the eyespot and the parafocal element. The self-similar configuration of the border symmetry system further suggests the essence of morphogenesis as the DCG cycle: repeated sequential events of epithelial distortions (D), calcium waves (C), and gene expression changes (G). Future studies should examine these hypotheses and speculations that constitute the induction model in butterfly wings and the generality of the DCG cycle in other organisms.

7.1 Introduction

One of the important goals of developmental biology is to understand how morphological structures are produced during development. Morphological structures are usually three-dimensional, but they are initiated as physical changes in a two-dimensional epithelial sheet to create three-dimensional bulges and dents. Developmentally speaking, the origin of morphology in amphibian embryogenesis can be traced back to the blastula stage, which is the stage when a sheet of cells emerges for the first time after fertilization. Subsequently, the plain cellular sheet undergoes dynamic cellular movement for gastrulation and eventually forms an embryo and, later, a complete adult individual. These processes are understood as mechanical changes of the epithelial cells. In this sense, a center of physical distortion forces could correspond to an organizing center. In insects, early embryogenesis is executed in the syncytial blastoderm, which may not be similar to this concept of mechanical changes, but a process of adult tissue formation from imaginal disks in the prepupal and pupal stages involves dynamic physical distortions of the epithelial cells.

In this view, morphogenesis can be considered to be a process of forming physical distortions over time through differential cellular contraction, adhesion between cells, and aggregation among cells and through cellular changes in size, shape, and number. Furthermore, the whole biological structure of a given organism can be viewed as a series of repetitions of epithelial distortions, despite their superficial dissimilarity. This kind of repetition unit may be called the "**morphogenesis unit**." Therefore, the mechanism employed to produce the morphogenesis unit is the essence of morphogenesis.

This view of morphogenesis has been derived from observations of diverse butterfly wing color patterns and from interpretations of physiologically induced color pattern changes (Otaki 2008a). Butterfly wings are mostly two-dimensional,

but careful examinations reveal that they are indeed three-dimensional (Taira and Otaki 2016), as in other tissues and organs in animals, and therefore likely involve mechanical forces that are generated by cellular changes in size, shape, and number. Butterfly wing disks at the larval and pupal stages are sheets of epithelial cells (more specifically, epidermal cells) that may be ready to accept mechanical changes. Butterfly wings additionally produce three-dimensional microstructures of scales and bristles, the processes of which are interesting but beyond the scope of this paper. In this paper, I endeavor to extract "the essence of morphogenesis" from the color pattern development of the border symmetry system. The border symmetry system is one of the symmetry systems in nymphalid color patterns and consists of border ocelli (eyespots) and parafocal elements (PFEs), which will be explained shortly below.

The repetition unit in biological entities may be identified by seeking homologous structures. **Serial homology** or **modularity** is a popular concept in the field of animal development. A good example of serial homology is serial eyespots on a single wing surface of nymphalid butterflies (Nijhout 1991; Beldade et al. 2002, 2008; Monteiro et al. 2003; Monteiro 2008, 2014). However, in this paper, I focus on **self-similarity**, a concept that is different from serial homology and modularity. Eyespots on a single wing surface are homologous but not self-similar; self-similarity is hierarchical repetition but not parallel repetition.

In the following sections, I first introduce the concept of self-similarity in biological entities using plants as examples. I use plants because they often manifest self-similar structures that are relatively easy to pinpoint, and many of them have been analyzed well mathematically (Mandelbrot 1983; Barnsley et al. 1986; Ball 1999, 2016).

7.2   Self-Similarity in Plants and Animals

In self-similar structures, a large structure contains its own smaller structures, wherein the small ones are nested within the larger one; they are hierarchically produced. In other words, the whole and its partial structures are similar to each other, but they are not necessarily morphologically identical in actual biological systems because of the extreme modifications of the essential process for their morphogenesis. These modifications often make identification of self-similarity difficult in actual biological systems.

One of the most famous self-similar structures in biological entities may be a fern or leaf structure that is produced by fractal branching patterns (Barnsley et al. 1986). Many leaves exhibit clear self-similarity, but the way it manifests is greatly dependent on the plants. A similar leaf branching pattern is also seen in bacterial growth (Ben-Jacob et al. 1994), blood vessels (Family et al. 1989), seaweeds, sponges and corals (Kaandorp and Kübler 2001), and other systems (Ball 1999, 2016), suggesting the universality of the branching fractal structures in biological systems.
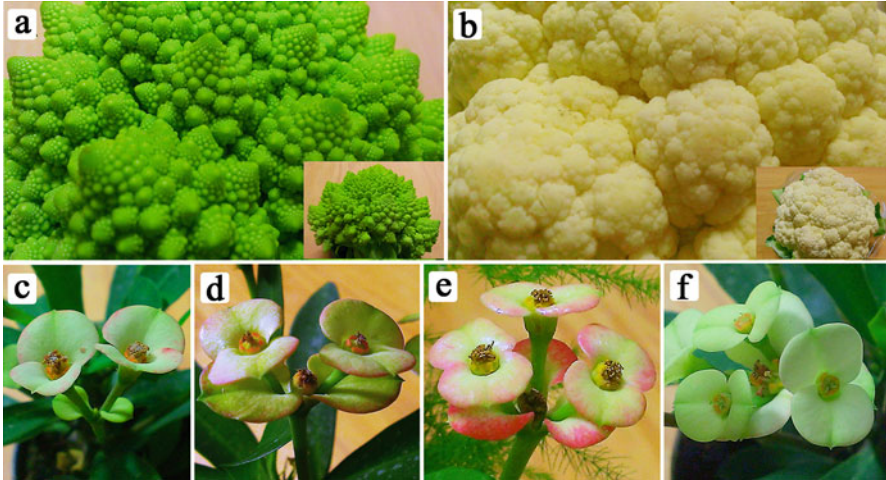
Fig. 7.1 Examples of self-similarity in plants. (**a**) Buds of cauliflower romanesco. An *inset* shows the whole structure. (**b**) Buds of a common cauliflower. An *inset* shows the whole structure. (**c–f**) Flowers of the crown of thorns, *Euphorbia milii*

The spiral floret arrangement of cauliflower romanesco (*Brassica oleracea var. botrytis*) is another famous example of self-similarity (Fig. 7.1a). A common cauliflower also exhibits self-similarity, but it is less clear (Fig. 7.1b). A similar spiral arrangement can be found in shells (Meinhardt 2009) and other systems (Ball 1999, 2016), suggesting that animals, too, have an ability to produce spiral fractal structures.

A more important and illuminating example salient to a discussion of butterfly color patterns can be found in the flowering pattern of *Euphorbia milii* (Fig. 7.1c-f). A single flower can produce a few smaller flowers from its own flower. This is a nested or hierarchical configuration, and these flowers are self-similar. It appears that this type of self-similarity in a complex biological entity (i.e., a flower in this example) that is not either simple branching or spiral patterns is relatively rare. A potential explanation for this finding is that the original self-similar structures are extensively modified to a degree unnoticeable by human eyes in most biological systems.

These examples in plants, animals, and other organisms demonstrate that organisms have an ability to form self-similar structures. I turn to butterfly wing color patterns from a viewpoint of self-similarity below, but before discussing self-similarity, I first discuss the symmetry in butterfly wing color patterns. Also in the following sections, I propose possible rules for color pattern formation in butterfly wings, which contain my own speculations. I then propose models and hypotheses that incorporate my speculations. For the readers' convenience, I summarize the color pattern rules at the elemental and sub-elemental levels that are discussed below in Table 7.1 and the additional color pattern rules at the scale and cellular levels in Table 7.2. I also summarize the models and hypotheses that are discussed in this paper in Table 7.3.

Table 7.1 Color pattern rules at the elemental and sub-elemental levels

1. Symmetry rule (color symmetry rule)	Pigment distribution is symmetric in a given system or element
2. Core-paracore rule	A unit of a symmetry system is composed of a single core element and a pair of paracore element
3. Self-similarity rule (nesting rule)	An eyespot and its accompanying parafocal element are self-similar
4. Binary rule (binary color rule)	Eyespot (and other elements) is depicted in dark color against light background color
5. Imaginary ring rule	An eyespot has a vanishingly weak light ring outside the outer-most dark ring
6. Inside-wide rule	In a full eyespot, the inner dark core ring (disk) is larger in width than the outer dark ring
7. Uncoupling rule	Sub-elements of an eyespot can be uncoupled from the rest of the eyespot
8. Midline rule	Center of a natural eyespot is placed at the midline of a wing compartment

Table 7.2 Color pattern rules at the scale and cellular levels

1. One-cell one-scale rule	A single scale cell produces a single scale throughout a butterfly wing
2. Color-size correlation rule for scales	Scales of elements (dark-colored scales) are larger than scales of background nearby (light-colored scales)
3. Central maxima rule for elemental scale size	Scales at the center of an element have the largest size in that element
4. Size-ploidy correlation rule for scales and cells	Scale size is correlated with the degree of ploidy of scale cells
5. Distortion rule for organizing centers	Organizing centers are physically distorted as bulges and dents that are reflected in pupal cuticle spots

7.3 Part I: Color Pattern Rules

7.3.1 Symmetry in Butterfly Wing Color Patterns

Highly diverse butterfly wing color patterns are thought to have been derived from a basic overall wing color pattern called the **nymphalid ground plan**. The nymphalid ground plan is a sketch of a general color pattern that was obtained by inductive reasoning from observations of many actual butterflies. This pattern was independently proposed by Schwanwitsch (1924) and Süffert (1927). Based on these two original schemes, a modern version was proposed by Nijhout (1991, 2001), and a few minor revisions were introduced by Otaki (2012a).

The nymphalid ground plan is composed of color pattern "**elements**," which are placed on a "**background**" (Fig. 7.2). The important point is that the elements are symmetrically arranged regarding pigment composition (i.e., coloration) (Nijhout

Table 7.3 Models and hypothesis for color pattern formation

1. Concentration gradient model (gradient model)	The classical model based on diffusive morphogen gradient that is released from organizing center. Thresholds are inherently set in signal-receiving cells
2. Transient models (collective)	Models that have been proposed transiently and withdrawn readily to investigate the simplest models for color pattern determination, including the two sub-step model and the multiple morphogen model
3. Adopted models (collective)	Models that have been proposed fragmentally but adopted to be synthesized as the induction model. Adopted models are the wave model, the two-morphogen model, and the heterochronic uncoupling model
4. Threshold change model	The most popular model that could explain color pattern modifications induced by physical damage and by pharmacological or temperature treatment
5. Induction model	An alternative model that proposes a sequential release of wavelike morphogenic signals from organizing center and dynamic interactions between signals
6. Rolling-ball model	A way of signal dispersion in the induction model, mainly based on the results of pharmacological modifications of parafocal elements and eyespots
7. Signal settlement mechanisms	A ways of signal settlement in the induction model. Three mechanisms are proposed: time-out mechanism, spontaneous velocity-loss mechanism, and repulsive velocity-loss mechanism. The latter has two sub-mechanisms: self-repulsive and nonself-repulsive velocity-loss mechanisms
8. Ploidy hypothesis	The hypothesis that morphogenic signal for color patterns is a ploidy signal. Scale color is determined as a result of cell size and the degree of ploidy
9. Physical distortion hypothesis	The hypothesis that morphogenic signal for color patterns is physical distortions of epithelial sheet
10. DCG cycle	The essence of morphogenesis in the revised version of the induction model, producing self-similar structures. D, distortion waves; C, calcium waves; G, gene expression

1994); this principle may be called the **symmetry rule** or, more accurately, **color symmetry rule**. In contrast, elemental shape is often very asymmetric. It has been believed that elemental symmetry in coloration comes from circular arrangements of morphogenic signals (signals that function as morphogens) from the organizing center located at the center of a prospective element.

There are three major symmetry systems (the basal, central, and border symmetry systems) and two peripheral systems (the wing root and marginal band systems) on the wings of nymphalid butterflies (Nijhout 1991, 2001; Otaki 2009, 2012a; Taira et al. 2015), although Martin and Reed (2014) stated reasonably that the basal
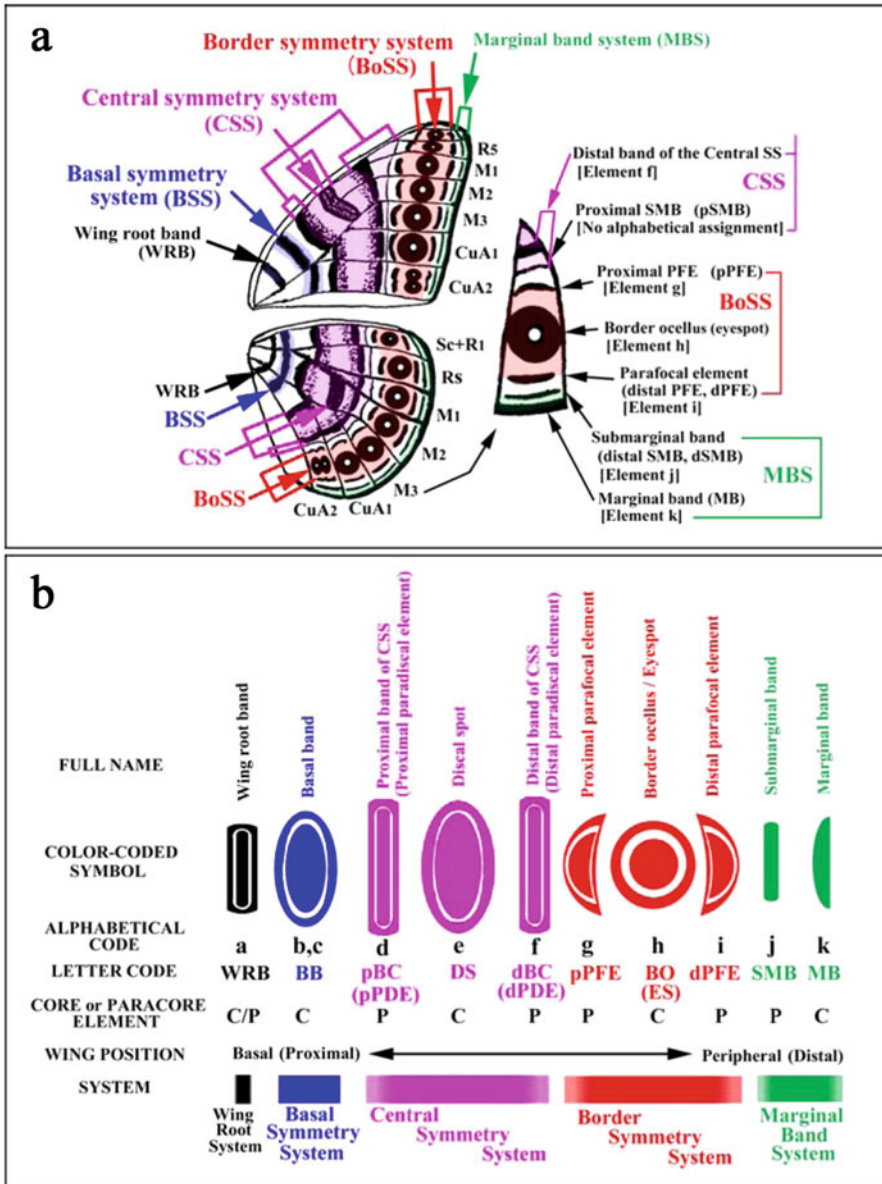
Fig. 7.2 The nymphalid ground plan. Reproduced and modified from Otaki (2012a) and Taira et al. (2015). (**a**) A standard scheme. In this scheme, dSMB is a part of the distal band of the central symmetry system (dBC) and thus may be omitted from the ground plan. (**b**) A simplified scheme. Elements are aligned from the basal (*left*) to the peripheral (*right*)

symmetry system may be associated with the central symmetry system. The two peripheral systems are also likely symmetric, but simply because they are placed at the wing margins, only a portion of them are expressed on a wing. It is likely that all five systems share the same developmental mechanism. In other words, they can be considered to have been derived from modifications of the basic "**ground pattern**" for a single symmetry system. In this sense, they are homologous. Importantly, it is reasonable to assume that each unit of a symmetry system is primarily organized by a single organizing center during development.

7.3.2   The Core-Paracore Rule and Self-Similarity Rule

Because eyespots and PFEs belong to the border symmetry system (Otaki 2009; Dhungel and Otaki 2009), it is likely that the unit of color pattern (or the basic "ground pattern") in any symmetry system of the nymphalid ground plan is composed of the **core element** and a pair of **paracore elements** (Otaki 2012a), which may be dubbed the **core-paracore rule**. The single elemental system containing the core and paracore elements is symmetric, and a single core element is symmetric regarding pigment composition. Likewise, a single paracore element is symmetric. Importantly, the pigment composition of a paracore element is often similar to that of a corresponding core element. Thus, the core-paracore rule may be elaborated as the **self-similarity rule (the nesting rule)**. Based on the core-paracore rule and the self-similarity rule, the diversity of the symmetry system can be understood as various modifications of the basic process of elemental formation (Fig. 7.3).

7.3.3   The Border Symmetry System and Its Self-Similarity

To understand the core-paracore relationship, I hereafter mainly focus on the border symmetry system in nymphalid butterfly wings. The core and paracore elements in this system are border ocelli (BOs or eyespots) and PFEs, respectively. PFEs are often found on the distal side of eyespots (dPFEs), and those on the proximal sides (pPFEs) are less frequent (Otaki 2009). When it is simply known as a parafocal element, dPFE is meant.

Examples of the border symmetry system are shown here. In *Argyreus hyperbius*, BOs and PFEs are both beige in color, although they have different shapes (Fig. 7.4a, left). In contrast, the submarginal bands are differently colored. This coloration pattern probably arises because BOs and PFEs belong to the same system, and they are different from submarginal bands, which belong to the marginal band system (Taira and Otaki 2016). In *Vanessa indica*, BOs and PFEs are similar both in coloration and shape (Fig. 7.4a, middle). In *Araschnia burejana*, PFEs are elongated oval rings with or without blue filling inside (Fig. 7.4a, right).
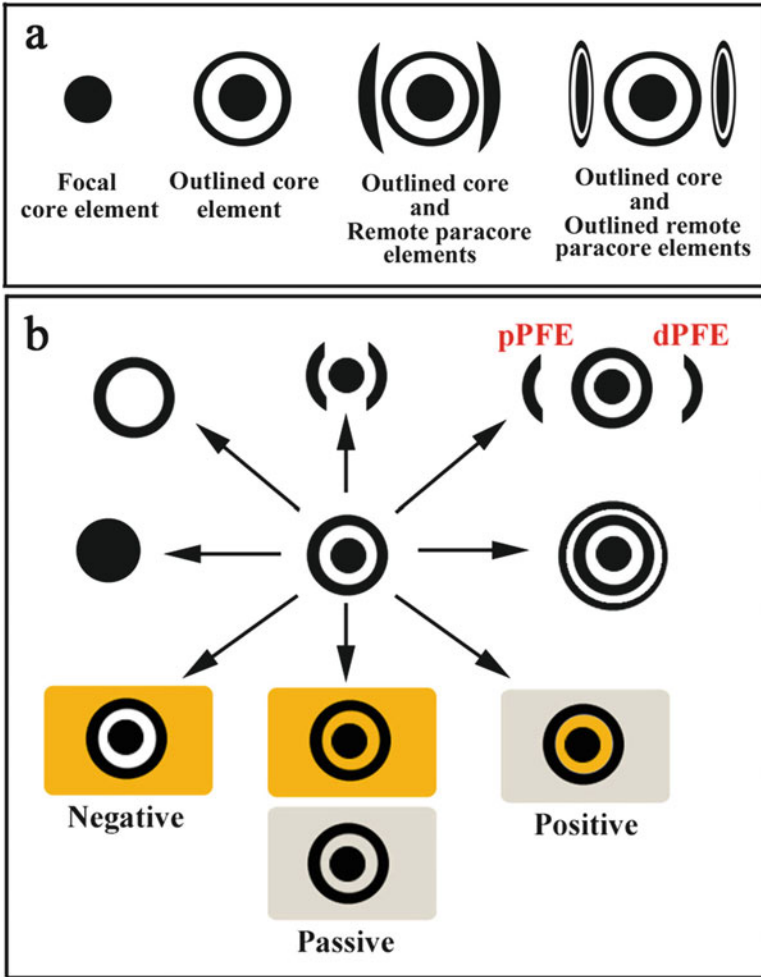
Fig. 7.3 Morphological transformation of color patterns of the border symmetry system Reproduced from Otaki (2012a). (**a**) Stepwise changes from the simplest black dot (*left*) to the complicated self-similar pattern (*right*). (**b**) Diverse transformation of a standard eyespot to various eyespots. Coloration of the inner light ring in a negative, passive, or positive fashion also contributes to eyespot diversity

This configuration of the border symmetry system appears to be typical in nymphalid butterflies.

Self-similarity between BOs and PFEs is not always clear in the cases above, but in *Tarattia lysanias*, the outer ring of a BO is isolated from the inner black disk, which is similar in shape to a PFE (Fig. 7.4b, left). The inner black disk of a BO is also divided into two rods in *Symbrenthia leoparda*, making a distinction in shape between BO and PFE difficult (Fig. 7.4b, right). Rod-shaped BOs and eyespot-
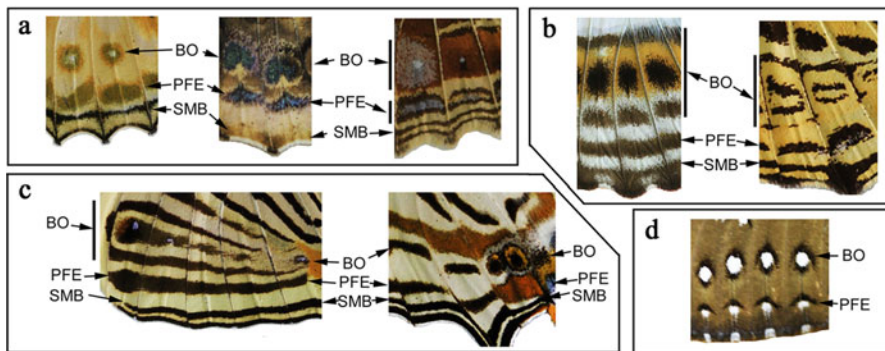
Fig. 7.4 Examples of the border symmetry system in nymphalid butterflies. BO, border ocellus; PFE, parafocal element; SMB, submarginal band. (**a**) *Argyreus hyperbius* (*left*), *Vanessa indica* (*middle*), and *Araschnia burejana* (*right*). (**b**) *Tarattia lysanias* (*left*) and *Symbrenthia leopard* (*right*). (**c**) *Colobura dirce* (*left*) and *Cyrestis camillus* (*right*). (**d**) *Hamanumida daedalus*

shaped BOs coexist on the identical wing surface in *Colobura dirce* and *Cyrestis camillus* (Fig. 7.4c). I believe, therefore, that a PFE is equivalent to an eyespot ring (Dhungel and Otaki 2009; Otaki 2009).

Another intriguing case is found in *Hamanumida daedalus*, where both BOs and PFEs are circular (not rod-shaped) and are similar to each other (Fig. 7.4d). This case strongly argues for self-similarity between BOs and PFEs.

7.3.4   Eyespot Pattern Rules: The Binary Rule and Inside-Wide Rule

To developmentally understand the symmetry rule, the core-paracore rule, and the self-similarity rule discussed above, additional rules regarding nymphalid butterfly color patterns will be discussed here.

An eyespot (BO) is composed of its parts, which may be called sub-elements. Typically, from the center to the peripheral regions, an eyespot is composed of a white dot, a dark (usually black) inner ring (disk), a light ring, and the outermost dark ring. Often, the light ring is variously colored, and the white dot may be absent. Additional rings may exist. The overall shape also varies from a near-true circle to extreme elongation such as rods and lines. Despite these diverse cases, the simplest eyespot is composed of two dark rings (inner and outer dark rings) and one light ring between them. Importantly, the light ring is similar or even identical to the background in coloration. That is, an eyespot is depicted in a dark color against a light background. This is called the **binary rule (binary color rule)** (Otaki 2011a). The binary rule can be revealed when BOs are expressed as rods or lines. *Symbrenthia leopard* (Fig. 7.4b, right) and *Colobura dirce* (Fig. 7.4c, left) illustrate this point: the light rings are continuous with the background, and they are colored

without any distinction from the background. The binary rule also implies that the outer dark ring (including PFE) is remotely located from the inner dark ring (disk). This means that morphogenic signals for the outer ring and PFE can travel long distances from the center of the symmetry system.

However, it is also true that in many eyespots, a light ring is not completely identical to the background but may be variously colored. I consider the light ring coloration to be evolutionary modifications. Because it is sandwiched by two dark regions, the light region has to have means to inhibit the invasion of black pigmentation during development. That is, I believe that the inhibitory signal is upregulated in the light ring. This inhibitory signal might have linked to pigment synthesis pathways later in evolution. The inhibitory signal also exists in the background region in contact with the outermost dark ring. This region often shows a vanishingly weak "light ring," which is called the imaginary ring (Otaki 2011b). This pattern may be dubbed the **imaginary ring rule**.

In nymphalid eyespots, the dark inner ring is almost always larger than the outer rings in width. This is called the **inside-wide rule** (Otaki 2012b). A "typical" eyespot without distortion that illustrates the inside-wide rule well can be found frequently in Satyrinae (Fig. 7.5a). Non-Satyrinae eyespots are likely more diverse but still largely follow the inside-wide rule (Fig. 7.5b). However, an exception to this inside-wide rule is small "immature" eyespots (Otaki 2011b), which were probably still developing when the signaling and reception steps were terminated (see below for the four-step process). Alternatively, inhibitory signals were upregulated earlier in the immature eyespot than in the mature eyespot (see
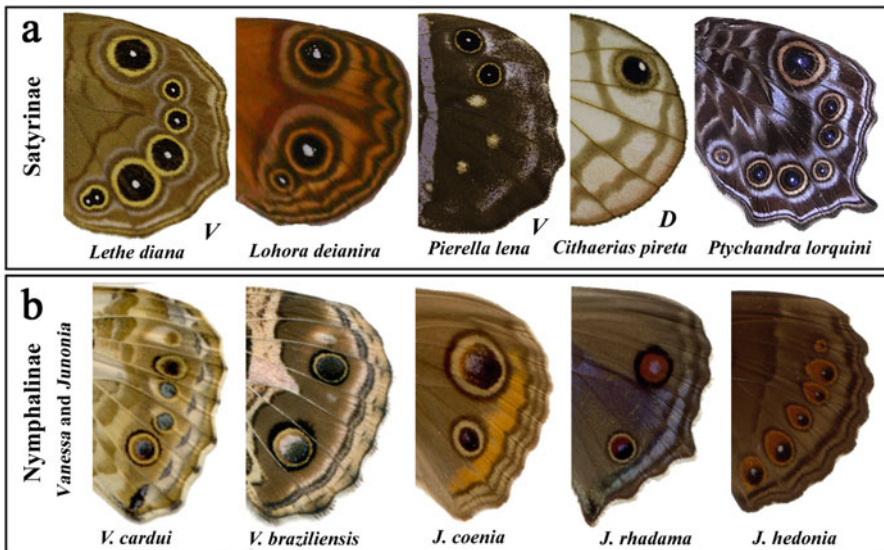
Fig. 7.5 Examples of nymphalid butterfly eyespots. (**a**) Satyrinae. (**b**) Nymphalinae

below for the induction model). These immature eyespots can be found among consecutive eyespots on a wing in many species (Fig. 7.5a, b).

The behavior of PFEs is worth mentioning. A PFE becomes larger when it is displaced toward the corresponding eyespot by pharmacological treatment (Otaki 2008a, 2012b), which follows the inside-wide rule. However, the PFE is sometimes larger than the entire BO, contrary to the inside-wide rule (if it is considered to be a part of an eyespot system as discussed above), as seen in *Argyreus hyperbius* (Fig. 7.4a, left). This exception probably occurs because, once moved away from the core element, the PFE behaves independently as a source of morphogenic signal, as the self-similarity rule suggests.

7.3.5 Eyespot Pattern Rules: The Uncoupling Rule and Midline Rule

An analysis of diverse eyespots indicates that the dark inner ring and the outer ring are not always placed on a single symmetry axis (Otaki 2011b). They appear to be independent of each other to some extent. This conclusion is also supported by physical damage experiments in which the outer ring enlarges and the inner ring diminishes in size in a single eyespot in response to damage (Otaki 2011c). Similarly, an eyespot white spot ("focus") behaves independently from the rest of the eyespot (eyespot body) (Iwata and Otaki 2016a). The uncoupling of the white spot is probably somewhat surprising for those who are not familiar with the genus *Calisto*, which has a white spot not at the center but outside an eyespot (Fig. 7.6). This type of semi-independent behavior of sub-elements is dubbed the **uncoupling rule**. The uncoupling behavior of sub-elements has been suggested in Nijhout (1990), Monteiro (2008), and Iwata and Otaki (2016a, b).

Despite the uncoupling, elemental centers are primarily located on the midline of a compartment (one of the Nijhout's design principles for formal models described in Nijhout (1990)); this may be called the **midline rule**. In contrast, damage-
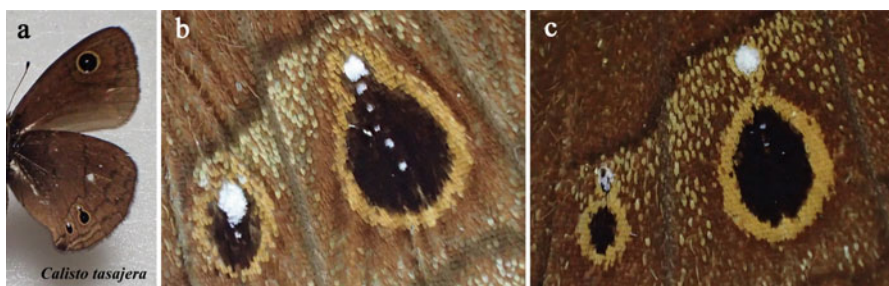
Fig. 7.6 Eyespots of *Calisto tasajera*. Reproduced and modified from Iwata and Otaki (2016a). (**a**) Ventral side of the whole wings. (**b, c**) Ventral hindwing eyespots of two different individuals. White spots are often located outside of the main eyespots in this species

induced elements can emerge at the non-midline (Otaki 2011c). Because the midline is defined by the wing veins, there is no doubt that the wing veins and compartments play critical roles in determining the location of a given element, as elaborated in Nijhout (1978, 1990, 1991).

7.4 Part II: Formal Models toward the Induction Model

7.4.1 Four Steps for Color Pattern Formation as a Starting Frame

It is first important to recognize as a starting frame that there are four sequential steps of color pattern formation: signaling, reception, interpretation, and expression (Otaki 2008a, 2012b). The signaling step was executed by organizing cells, whereas the other three steps were executed by immature scale cells that receive positional information. Most models, including the induction model below, focus on the signaling step and do not pay much attention to the latter three steps. However, the diversity of actual butterfly color patterns may be realized by changes in any single step, at least theoretically.

7.4.2 Gradient Model for Positional Information

The **concentration gradient model** for positional information is probably still the most popular model to explain butterfly eyespot formation (Nijhout 1978, 1980a, 1981, 1990, 1991; French and Brakefield 1992, 1995; Brakefield and French 1995; Monteiro et al. 2001). However, the gradient model cannot easily explain the pattern rules discussed above. Furthermore, it is difficult to explain the additional features of diverse color patterns in actual butterfly wings such as multiple dark rings and differences between small and large eyespots that have drastically different morphology in adjacent compartments using this model (Otaki 2011a, b). Additionally, this model cannot explain dynamic signal interactions (Otaki 2011a, b, c). Time series of color deposition in pupal wings have revealed that red color for an eyespot light ring that develops earlier is "overwritten" by black color that develops later and that a given black area develops as a fusion of patchy black islands (Iwata et al. 2014). These ontogenic observations are not compatible with the gradient model.

However, these facts do not completely deny the usefulness of the gradient model. I believe that a concentration gradient of signaling molecules may play an important role in finalizing the expression of genes for pigment synthesis in a relatively short range (e.g., within a given eyespot ring) (see below). In this sense, gene expression changes may be a result (not a cause) of upstream long-range signals from the center of a prospective eyespot.

7.4.3   Transient Models for TS-Type Modifications and Parafocal Elements

Although I mentioned that the conventional gradient model was not satisfactory, I did not immediately reach this conclusion; I devised a few models before the induction model. I here collectively call them **transient models** because they were transiently proposed and readily discarded. Nonetheless, these models are important to determining the simplest (most parsimonious) model that reasonably explains experimentally induced and naturally occurring eyespots and PFEs. The inclusion of PFEs in the process of making a formal model is critical because both eyespots and PFEs belong to the same symmetry system.

To explain the PFE formation in eyespot-forming and eyespot-less compartments based on the gradient model, the two sub-step model for eyespots and PFEs has been proposed (Otaki 2008a). In this model, a diffusive gradient is first formed to determine the location of PFEs in both eyespot-forming and eyespot-less compartments. After the determination of the PFE location by the periphery of the gradient, the gradient entirely disappears quickly and does not form an eyespot in an eyespot-less compartment. Note that the presence and absence of an eyespot cannot be attributed to threshold differences between the two compartments because they have the same threshold levels if the thresholds exist at all, as shown in an eyespot that occupies two or more compartments (Otaki 2011b). This two sub-step model should also mean that the reception step first takes a snapshot of the PFE, and after the disappearance of the eyespot signal, another snapshot should be taken. This model is too awkward to be accurate, but it hints at the importance of uncoupling the behavior of the PFE from the eyespot proper.

Multiple morphogens (and multiple receptors) for PFEs and eyespots may also save the gradient model. In this multiple morphogen model, there are a few different chemicals that act as morphogens. This model explains a difference between the eyespot-forming and eyespot-less compartments. That is, a morphogen for a PFE is secreted in both compartments, but a morphogen for an eyespot is not secreted in an eyespot-less compartment. However, considering that the PFE is equivalent to the outer eyespot ring belonging to the border symmetry system, multiple morphogen factors are not likely. The introduction of multiple factors in a model can produce all-around models but violates the parsimony of model construction.

Despite these efforts, it is better to abandon the idea of the gradient model, considering its difficulty in explaining the color pattern rules and other points discussed in the previous section. An alternative model is the wave model, in which the signal is transmitted as a series of waves (Otaki 2008a). In this context, the two sub-step model discussed above may be modified to support the wave model, in which the first morphogen for a PFE is released as the first wave and the second morphogen is released as the second wave for the eyespot (more precisely, as the second wave for the eyespot outer ring and then as the third wave for the eyespot inner ring) (Otaki 2008a; Dhungel and Otaki 2009). In this two-morphogen

model (wave model), two (or three) morphogens are identical in chemical (or physical) qualities (and therefore different from multiple chemical factors) but are released heterochronically as a train of pulses, being consistent with the heterochronic uncoupling model for TS-type changes (see below). These two models (the wave model and the two-morphogen model) have not been discarded. Rather, they have been adopted, together with the heterochronic model below, and synthesized as the induction model. They may collectively be called the **adopted models**.

There is a weakness in this wave model (Otaki 2008a). Focal damage produces a smaller-than-usual eyespot, indicating the source dependence of the signal. In general, wave signals are not source dependent, theoretically. However, the results of damage experiments can be explained well by the revised version of the induction model (see below).

7.4.4 Heterochronic Uncoupling Model for TS-Type Changes

I have examined the color pattern modifications induced by temperature shock or pharmacological treatments (collectively called the TS-type modifications) (Hiyama et al. 2012; Otaki and Yamamoto 2004a, b; Otaki et al. 2005b, 2006, 2010; Otaki 2007, 2008b, c; Mahdi et al. 2010, 2011) (Fig. 7.7a). It is worth noting that temperature treatments (Nijhout 1984) and pharmacological treatments (Otaki 1998, 2008a; Serfas and Carroll 2005) are the only means that can efficiently create
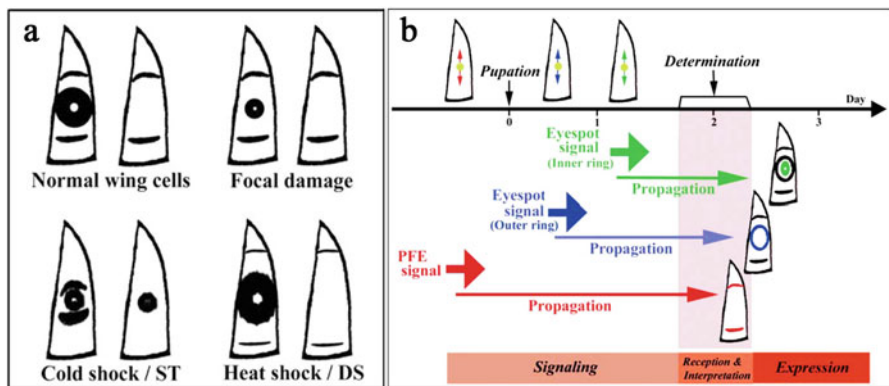
Fig. 7.7 Effects of physiological treatments on eyespot and parafocal element. Reproduced and modified from (Otaki 2011a). (**a**) Modification patterns of various treatments. Two wing compartments (one with an eyespot and a parafocal element and the other with a parafocal element only). ST and DS indicate treatment with sodium tungstate and dextran sulfate, respectively. (**b**) Interpretation of the modifications. Signals are released in the order parafocal element, eyespot outer ring, and eyespot inner ring

this "artificial rearrangement of elements" or "elemental transformation," which is reminiscent of evolutionary trial and error to invent new color patterns based on the nymphalid ground plan. These color pattern modifications are evolutionarily and physiologically relevant (Hiyama et al. 2012; Otaki and Yamamoto 2004a, b; Otaki et al. 2005b, 2006, 2010; Otaki 2007, 2008b, c; Mahdi et al. 2010, 2011), justifying their use as an important method to construct a formal model. The **threshold change model** is the most popular interpretation of the TS-type modifications (Otaki 1998, 2008a; Serfas and Carroll 2005) as well as of physically induced modifications (Nijhout 1980a, 1985; French and Brakefield 1992, 1995; Brakefield and French 1995). However, the TS-type modifications cannot be reproduced by simple threshold changes, as not only relative locations but also the size and colors of the elements are changed. For example, modifications of PFE in an eyespot-less compartment often produce eyespot-like spots (Otaki 2008a).

Because the TS-type modifications are interpreted as a series of possible color pattern snapshots during development, the modifications are likely consequences of a delay of the signaling step (slow signal propagation) or an acceleration of the reception step (Otaki 2008a). That is, temperature shock and pharmacological treatments introduce a time difference between the signaling and reception steps, leading to the heterochronic uncoupling model for TS-type changes. This model simply notes that the TS-type modifications are products of snapshots of propagating signals, which is part of the basis of the induction model (Fig. 7.7b).

7.5 Part III: Induction Model

7.5.1 An Overview

To be consistent with the color pattern rules discussed in Part I above and to reflect a few relevant models discussed in Part II, an integrated model is required. To this end, I have proposed the **induction model** (Otaki 2011a, 2012b). This model is largely based on the "movement" of PFEs and eyespots by tungstate injection and other physiological treatments (Fig. 7.7a). In other words, the induction model is not based on the putative diffusive molecule, which is in contrast to the gradient model.

The physiological modifications can be interpreted as follows, which is indeed a simplified version of the induction model to explain a determination process of the border symmetry system (Fig. 7.7b). Signals for PFEs, the outer ring, and the inner ring are released independently in this order with defined intervals, and each signal propagates independently. These signals are simultaneously received by immature scale cells at the reception step.

7.5.2 Early and Late Stages

The induction model can be separated into many steps but roughly into two stages: the early and late stages (Fig. 7.8a). The early stage is the primary signal expansion and settlement. The late stage is the induction of activating signals (and their self-enhancement) and inhibitory signals and their stabilizing interactions. The late stage of the induction model employs the concept of "the short-range activation and long-range lateral inhibition" (Fig. 7.8b), which is the core concept of the reaction-diffusion model (Gierer and Meinhardt 1972; Meinhardt and Gierer 1974, 2000; Meinhardt 1982). In the induction model, the dark and light areas in an eyespot correspond to the areas of activator and inhibitor signals, respectively.

In contrast, the early stage does not follow the reaction-diffusion mechanism because the method of signal propagation is different; the signal is thought to be propagated according to the **rolling-ball model** (Otaki 2012b). The signal behaves like numerous minute balls rolling on a board of even friction (constant deceleration) (Fig. 7.9a). This behavior is described by classical mechanics. The propagation is thus determined by the initial velocity of each minute unit signal. In addition, the interval of signal release determines the overall shape of an eyespot. The signals propagate slowly and gradually slow down. These properties of signals satisfy the binary rule and the inside-wide rule and produce natural and experimentally induced eyespots and PFEs. These properties also satisfy the uncoupling and heterochronic nature of the signal. It is also possible to simulate morphological differences between small and large eyespots (Fig. 7.9b).

7.5.3 Settlement Mechanisms

In the induction model, there are different modes of **signal settlement** that are proposed (Otaki 2012b). First, a snapshot of propagating signals may be taken by the transition from the signaling to reception steps (the time-out mechanism). Second, propagating signals stop when velocity is lost spontaneously because of low initial velocity (spontaneous velocity-loss mechanism) and when the propagation is blocked by an inhibitory signal nearby (repulsive velocity-loss mechanism). The repulsion comes not only from a nearby element (non-self-repulsive velocity-loss mechanism) but also from the signals for the imaginary ring (the outermost inhibitory ring that is not well expressed) that are induced by the outermost dark ring (self-repulsive velocity-loss mechanism). In this sense, the speed and level of the inhibitory signal induction primarily determine the final size of an eyespot. The self-repulsive mechanism thus ensures autonomous determination of an eyespot.

Fig. 7.8 Induction model for positional information. Reproduced from Otaki (2011a). (**a**) Sequential steps of eyespot formation. (**b**) Short-range activation and long-range inhibition in the late stage of the induction model
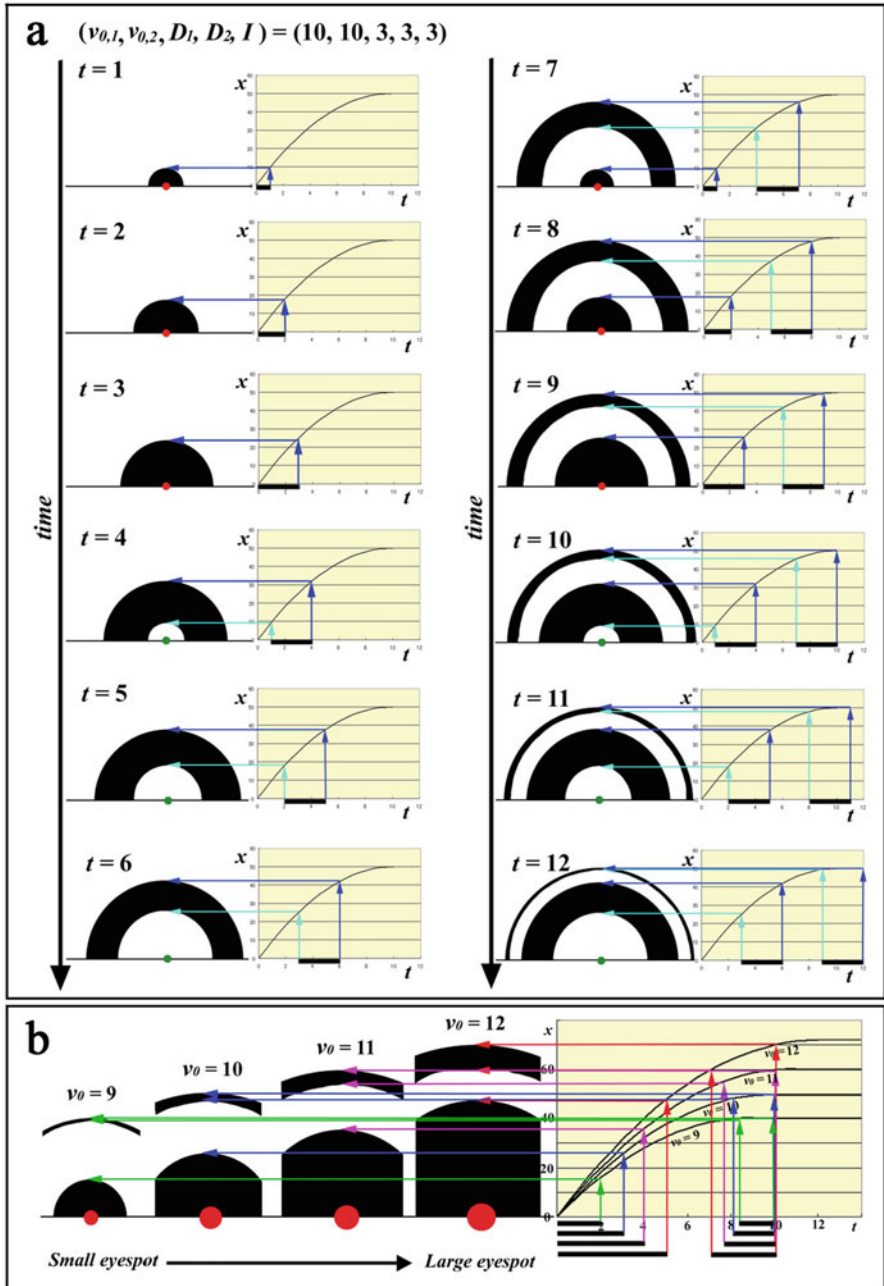
Fig. 7.9 Simulation of eyespot formation based on the rolling-ball model. Reproduced from Otaki (2012b). (**a**) Time course of developmental signals for a typical eyespot. The signals follow the curve shown on the right side of each time point. Initial velocity (v_0) and signal duration (D) are set for two black rings together with their signal interval (I). (**b**) Effect of various initial velocities (v_0). Various eyespots are produced

7.5.4   Mechanisms for Self-Similarity

There should be a mechanism that produces self-similar structures, which is based on the following mechanism: highly enhanced activating (black-inducing) signals in the late stage would signify a new organizing center. This mechanism can be explained by the ploidy hypothesis (Iwata and Otaki 2016b), which states that the morphogenic signal for color patterns is indeed a ploidy signal that induces polyploidization and cellular size increase (see below), together with the physical distortion hypothesis, which states that cellular and epithelial distortions act as morphogenic signals (see below). The origin of distortions can be considered as organizing centers. Importantly, the self-similarity of eyespots and PFEs argues for the repulsive velocity-loss mechanism and against the time-out mechanism because the signal dynamics should still persist after the possible time-out for the primary organizing centers for eyespots, when the secondary organizing centers for parafocal elements are determined and become activated. That is, the time-out mechanism cannot explain the heterochronic behaviors of the primary and secondary signal dynamics.

7.5.5   Reality Check

Is there any signal that can follow the rolling-ball model in biological systems? In the mesoscopic world (not microscopic world explained by quantum physics nor macroscopic world explained by classical mechanics) of cells and molecules in water, Brownian motion and non-covalent molecular interactions prohibit the rolling-ball-like behavior of a molecule. In contrast, mechanical force can be transmitted easily via an epithelial sheet if epithelial cells are connected firmly but flexibly. That is, epithelial distortions may show rolling-ball-like behavior and act as morphogenic signals from organizing centers. In Part IV below, I review evidence for the ploidy hypothesis and the distortion hypothesis.

7.6   Part IV: Ploidy, Calcium Waves, and Physical Distortions

7.6.1   Scale Size of Elements

At the cellular level, one cell builds one scale (Nijhout 1991), which may be dubbed the **one-cell one-scale rule.** Therefore, any morphological features of scales directly indicate the developmental status of the scale-building cells (or simply scale cells). Scale size distribution is graded from the basal to peripheral areas of a wing in butterflies and moths (Kristensen and Simonsen 2003; Simonsen and

Kristensen 2003). Similar size gradation has been found in the background scales in *Junonia orithya*, *J. almana*, *Vanessa indica*, and *V. cardui* (Kusaba and Otaki 2009; Dhungel and Otaki 2013; Iwata and Otaki 2016b).

What about the size of scales that constitute elements? In *J. orithya* and *J. almana*, the scale size of an element is larger than that of its surrounding background (Kusaba and Otaki 2009; Iwata and Otaki 2016b) (Fig. 7.10). In this sense, scale color and size are reasonably correlated, which can be called the **color-size correlation rule for scales**. This rule may sound trivial but is indeed important as a clue to understanding the possible nature of morphogenic signals for color patterns (see below). Furthermore, the largest scales in an element are found roughly at the center of an element (Kusaba and Otaki 2009; Iwata and Otaki 2016b). This may be called the **central maxima rule for elemental scale size**. It is important to recognize that scale size changes suddenly at the boundary between the inner black ring of an eyespot and a yellow ring. There are similar abrupt changes at the outer ring boundary and the PFE boundary. These abrupt size changes may reflect the independence of black areas (the binary rule and the uncoupling rule) rather than gradual changes of positional information.

Additionally, scales of different colors differ in their structure, such as overall scale shape and scale ultrastructure (Gilbert et al. 1988; Nijhout 1991; Janssen et al. 2001). Our laboratory also obtained similar results using *Junonia* and other butterflies (Kusaba and Otaki 2009; Iwata and Otaki unpublished data; Kazama et al. 2017).
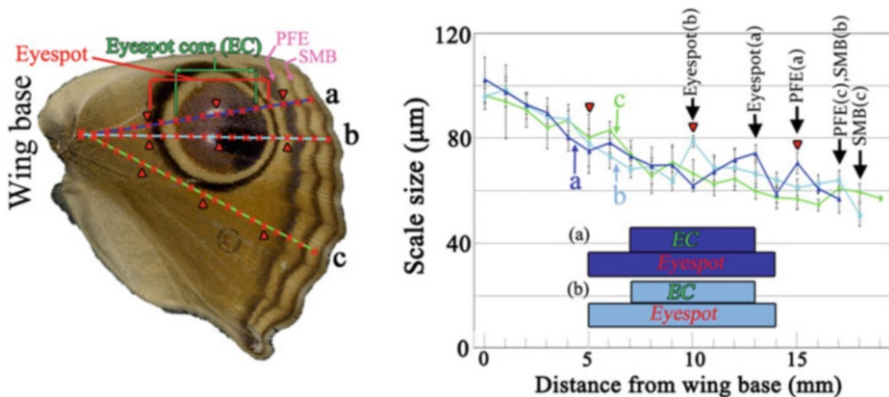
Fig. 7.10 Scale size distribution on a wing of *Junonia almana*. Reproduced from Iwata and Otaki (2016b). A dorsal forewing was examined along lines *a*, *b*, and *c* in 1.0 mm intervals (*left*). Results are shown in the graph (*right*). Along line *b*, scale size peaked at the center of the eyespot. Along line *a*, the peak was located at the distal edge of the eyespot core and also at the center of the parafocal element (PFE). Line *c* did not show conspicuous peaks. All lines showed the size decrease from the basal to the peripheral areas except at the elemental positions

7.6.2 Ploidy Hypothesis

According to Henke (1946) and Henke and Pohley (1952), scale size reflects the degrees of ploidy of the cell in moths (Sonhdi 1963; Cho and Nijhout 2013). This size-ploidy relationship, or the **size-ploidy correlation rule for scales and cells**, is probably applicable to butterflies. This leads us to propose the **ploidy hypothesis** (Fig. 7.11a) (Dhungel and Otaki 2013; Iwata and Otaki 2016a, b). This hypothesis states that morphogenic signals induce polyploidization of signal-receiving cells. The higher the ploidy level, the larger the cell. The larger the cell, the larger the scale it can produce. Simply because a high ploidy level means high numbers of genes for pigment synthesis enzymes, the concentration of pigment in the scales can
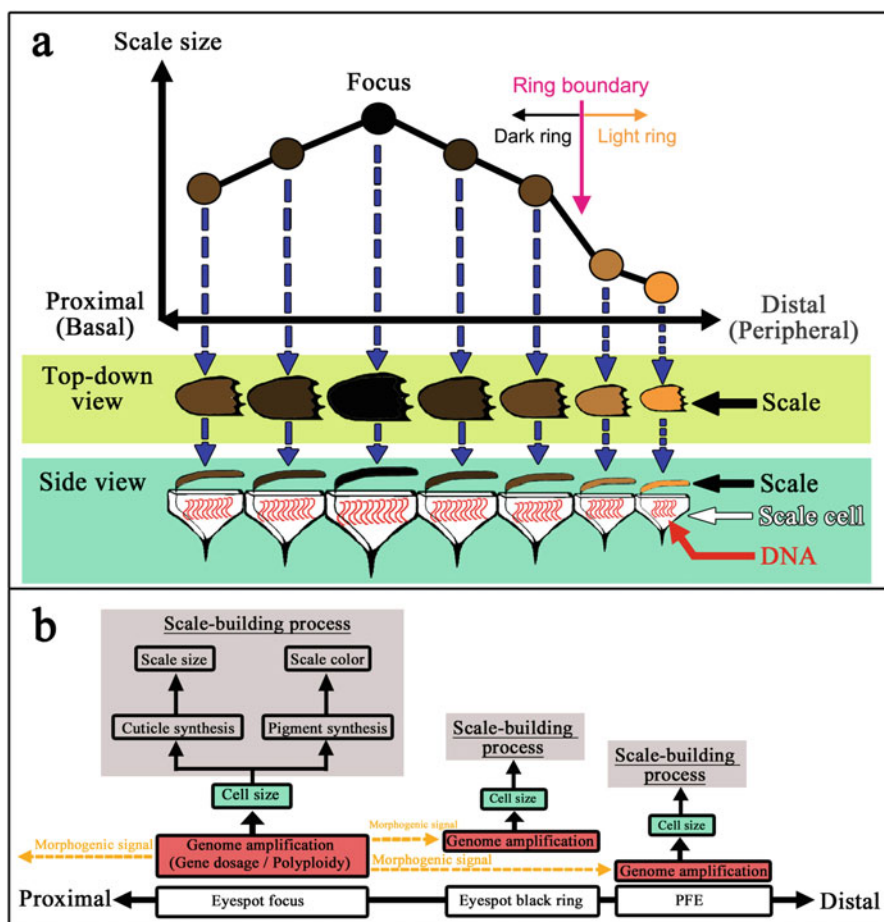
Fig. 7.11 Ploidy hypothesis. Reproduced from Iwata and Otaki (2016b). (**a**) Scale size distribution and its relationship with cell size. (**b**) A hypothetical determination process for scale color and size based on the induction model

change their coloration. Alternatively, gene dosage determines which pigment to be synthesized. In this way, the level of morphogenic signals indirectly determines the levels of pigment chemicals in a scale through the regulation of polyploidization or gene dosage. The ploidy hypothesis is an important component of the induction model (Fig. 7.11b).

The recent discovery that a cell cycle regulator, *cortex*, plays a role in the darkening of the wings in butterflies and moths (Nadeau et al. 2016; van't Hof et al. 2016) may be a surprise for many biologists, but this discovery fits well with the ploidy hypothesis, although it is not discussed in these papers. This cell cycle regulator may control a process of polyploidization of immature scale cells, which determines the final coloration of scales according to the ploidy hypothesis.

7.6.3 Calcium Waves

Recently, spontaneous long-range calcium waves have been discovered in the developing pupal wings *in vivo* (Ohno and Otaki 2015b). Calcium waves have been found to be released from the prospective eyespot centers and from damage sites (Fig. 7.12), although wave origins are not restricted to known elemental centers. At least four different types of waves are observed: expanding ring or traveling line, wandering line or point, oscillating area, and traveling oscillating area. Color patterns are disrupted by the injection of thapsigargin, a well-characterized inhibitor of Ca^{2+}-ATPase in the endoplasmic reticulum. For example, fuzzy boundaries of pattern elements have been reported in thapsigargin-treated individuals (Otaki et al. 2005b; Ohno and Otaki 2015b). I speculate that the calcium waves act as the activator in the late stage of the induction model, but calcium waves are not morphogenic signals themselves. Morphogenic signals are likely to be physical distortions (see below), and calcium waves may be released from these distortion waves.

7.6.4 Physical Distortion Hypothesis

What are the morphogenic signals? Despite the prediction of the rolling-ball model, it is difficult to imagine numerous minute "balls" rolling out from the center of a prospective eyespot. A hint comes from a study on pupal cuticle spots and their associated structures. Remarkably, organizing centers are often marked inherently as pupal cuticle focal spots in butterflies (Nijhout 1980a, b, 1990, 1991; Otaki et al. 2005a; Taira and Otaki 2016) (Fig. 7.13). This feature is especially notable in *Junonia* butterflies, but it is widely seen in many nymphalid butterflies that have eyespots or black spots (Otaki et al. 2005a). In addition, some cuticle focal spots are accompanied by cuticle marks. These spots and marks are likely produced by organizing cells for adult eyespots. The epithelial distortion structures of the
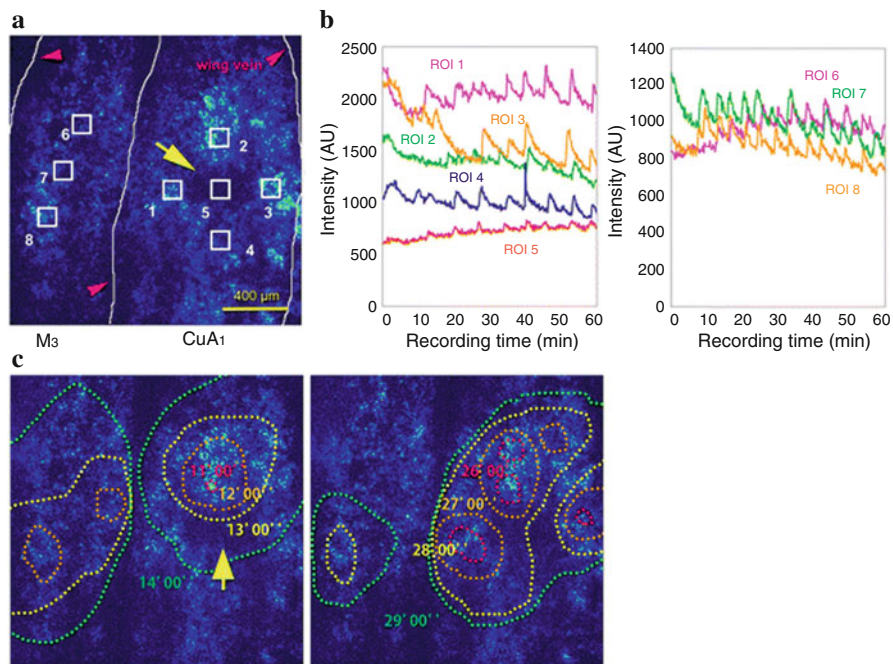
Fig. 7.12 Spontaneous calcium waves from the prospective organizing center for eyespot. Reproduced and modified from Ohno and Otaki (2015b). (**a**) Calcium signals (*blue*) in the M_3 and CuA_1 compartments. ROIs 1–8 were examined for intensity changes in the following panels. The *yellow arrow* indicates the prospective eyespot (also in **c**). The *red arrowheads* indicate the wing veins. (**b**) Fluorescence intensity changes of Fluo-4 in ROIs. (**c**) Propagating calcium signals around the prospective eyespot area. Panels in **a** and **c** show a single identical visual field at different time points. The shape of a wave at a given time point (in min) is depicted by a *dotted circle*

prospective elements have also been confirmed by *in vivo* imaging of the living tissue (Ohno and Otaki 2015a; Iwasaki et al. 2017). The association of the organizing centers with distortion structures may be called the **distortion rule for organizing centers**.

It is likely that the cellular volume increase or change in shape at the particular position results in the formation of the pupal cuticle spot as a by-product. The cellular changes would cause epithelial distortions, which could expand as a series of waves. The slow contraction of the wing tissue during the early pupal stage revealed by time-lapse movies (Iwata et al. 2014) probably helps to expand the distortion waves. That is, the **physical distortion hypothesis** states that morphogenic signals are physical distortions of an epithelial sheet. The distortion hypothesis thus states that morphogenic signals cannot be reduced to a substance. Rather, these signals are a wave, i.e., a physical phase change of a medium (the epithelial sheet). To realize this signaling system, the epithelial sheet has to have a tension or at least cellular connections in some way, which is likely the case (Ohno and Otaki
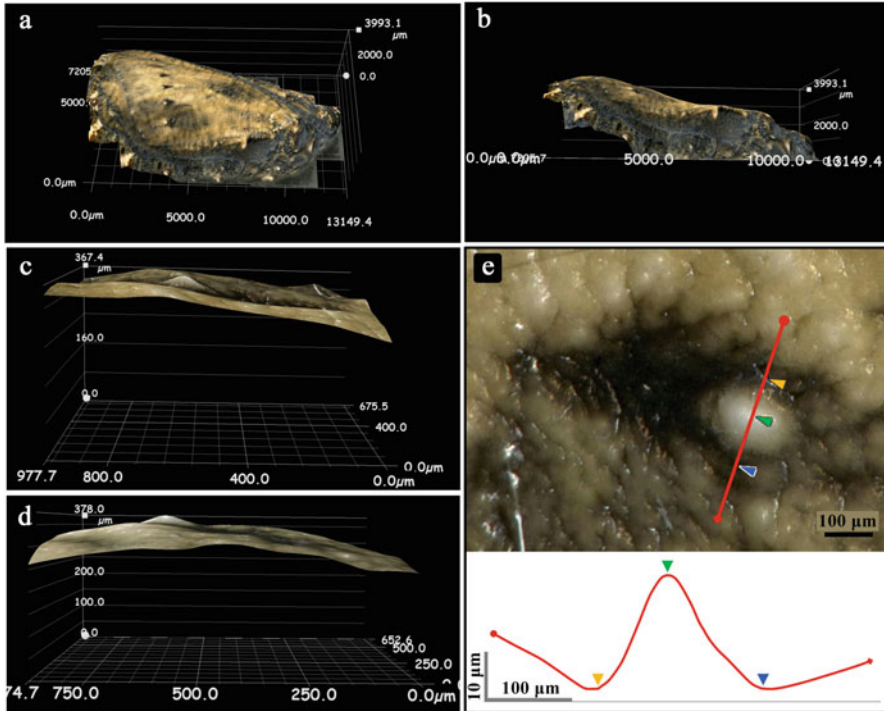
Fig. 7.13 Pupal focal cuticle spot of *Junonia orithya* based on three-dimensional reconstruction. Reproduced from Taira and Otaki (2016). (**a**) Top-down view of the entire left forewing surface. (**b**) Side view. (**c, d**) A pupal cuticle spot. (**e**) High-magnification image of a pupal cuticle spot and its cross-sectional height. *Colored arrowheads* in the image indicate the site of measurement in the graph

2015a). A physical distortion could open stretch-activated calcium channels, as in other systems (Lee et al. 1999; Tracey et al. 2003; O'Neil and Heller 2005; Hillyard et al. 2010). Epithelial cells that have received enough calcium ions inside could duplicate their genome and differentiate into scale cells that harbor specified cell size and specified scale size. In this time series, gene expression changes are downstream (not upstream) events; in other words, these changes are not a cause but a result of morphogenic signal propagation.

The distortion hypothesis states that mechanical disturbance of an epithelial sheet functions as morphogenic signals. This idea may sound unfamiliar to biologists, but this should not be a reason to reject this model as long as the model is consistent with experimental and observational results. Fortunately, mechanobiology is an expanding interdisciplinary field between biology and physics (Iskratsch et al. 2014). Changes in the mechanical property of a cellular sheet may be caused by physical damage and subsequent wound-healing processes (Antunes et al. 2013) and by cell death (Teng and Toyama 2011; Toyama et al. 2008) in addition to cellular size and shape changes.

7.6.5   Damage-Induced Ectopic Elements

Physical damage at the prospective eyespot center immediately after pupation has been shown to reduce or eliminate eyespots, but damage at the prospective background induces ectopic elements in butterfly wings (Nijhout 1985; Brakefield and French 1995; French and Brakefield 1992, 1995; Otaki et al. 2005a, b; Otaki 2011c). Ectopic eyespots are most likely by-products of a wound-healing process. I believe that physical damage elicits physical distortions of the epithelial sheet. Interestingly, the genes expressed are similar in normal development and in the healing process (Monteiro et al. 2006). Likewise, physical damage elicits calcium waves in normal development and in the healing process (Ohno and Otaki 2015b). Thus, the wound-healing process and the normal process of color pattern development would share similar mechanisms not only at the phenotypic level but also at the molecular level.

If the putative morphogen from a natural organizing center is a specific substance, it is difficult to imagine that physical damage confers an ability in immature epithelial cells to synthesize that specific substance. Probably partly for this reason, it is often interpreted that physical damage (and also pharmacological treatments) increases or decreases the "preset" threshold levels of signal-receiving immature scale cells in the conventional gradient model (Nijhout 1985; Brakefield and French 1995; French and Brakefield 1992, 1995; Otaki et al. 2005a, b; Otaki 2011c). Although it is entirely possible that this interpretation explains many damage-induced effects, dynamic interactions between two adjacent eyespots during development, shown in *J. almana*, suggest that a simple change in threshold levels is not realistic; when one eyespot becomes smaller as a result of damage, the other eyespot becomes larger (Otaki 2011c). It should also be noted that a possible mechanism of how damage lowers threshold, if this is the case, has never been well explained.

7.6.6   Focal Damage

What will occur when physical damage at the eyespot focal site is elicited? At the early stage of pupae, a smaller-than-normal eyespot is produced. Interestingly, late damage produces a larger-than-normal eyespot. The late damage result is explained by the addition of a new signal because this is similar to the fact that background damage produces a new signal for an eyespot or a black spot. The early damage result is explained as the damage of the signal-producing cells, resulting in the low-level signal. However, this result may indicate the source dependence of the signal, whereas wave signals are supposed to be source independent.

Considering the physical distortion hypothesis, the focal damage during the signal release may simply relax the distortion of the epithelial sheet. As a result, a distortion wave cannot go away. It may even go back to the original state. In contrast, at the later stage, epithelial distortions may have already been relaxed and

the signal is ready to settle. Thus, the late focal damage may recreate the distortion, such as the background damage, resulting in a larger-than-normal eyespot.

7.7 Part V: Generalization and Essence

7.7.1 Reinforced Version of the Induction Model

To summarize, the reinforced version of the induction model for eyespot development is explained below (Fig. 7.14). This scheme includes many speculations to bridge the fragmented knowledge of the butterfly wing system. For simplicity, the development of a simple black disk (i.e., black spot) is delineated first below (Fig. 7.14a).
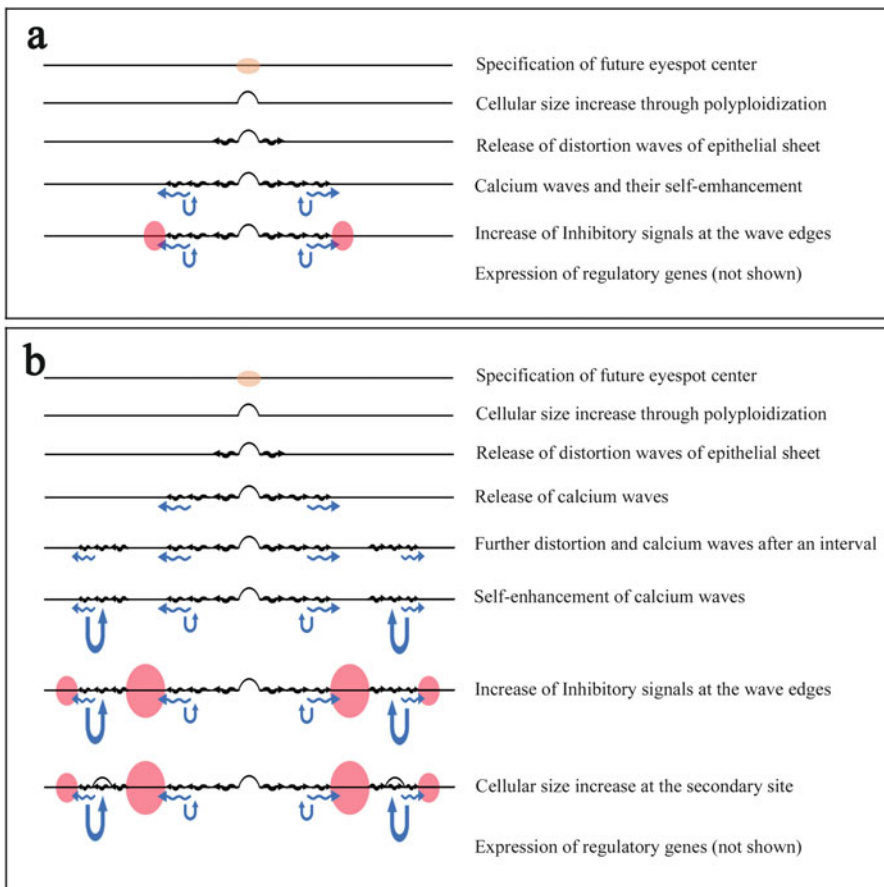
Fig. 7.14 Reinforced induction model. Time series of events from the top to the bottom. (**a**) Black spot formation. (**b**) Eyespot formation

In the beginning, a future eyespot center (organizing center) is first specified. Physical distortion of the epithelial sheet is formed due to cellular size changes and deformations. These cellular changes would cause distortion waves that propagate radially to surrounding cells, according to the rolling-ball model. The propagating waves are "translated" into chemical signals, i.e., calcium waves, possibly through a stretch-activated calcium ion channel on the membrane, acting as an activator in a reaction-diffusion model, as traveling calcium waves have been detected (Ohno and Otaki 2015b). As the physical distortions and their associated calcium signals propagate, calcium signals may be enhanced by themselves as oscillations, as oscillating calcium waves have also been detected (Ohno and Otaki 2015b). Calcium oscillations induce unknown inhibitory signals in cells located in the periphery of the oscillations. The induced inhibitory signals inhibit further propagation of the original calcium signals, finalizing the position and shape of the black spot. Calcium oscillations stimulate cells to undergo genome amplification and to express a set of regulatory genes such as *Wnt*-family genes (Monteiro et al. 2006; Martin and Reed 2014), *spalt* and *Distal-less* (Monteiro et al. 2013; Adhikari and Otaki 2016; Dhungel et al. 2016; Zhang and Reed 2016). Alternatively, calcium oscillations may be stabilized by the Wnt/Ca^{2+} transduction pathway that involves intracellular calcium release (Kühl et al. 2000; Kohn and Moon 2005). Cellular size increases in the prospective black ring according to the genome size or ploidy level. This process may be regulated by the *cortex* gene, which has been identified recently (Nadeau et al. 2016; van't Hof et al. 2016). The final cellular size or the degrees of polyploidy then determine a repertoire of pigment synthesis genes to be expressed.

When an eyespot is produced, the scheme is more complicated (Fig. 7.14b). A released distortion wave does not readily induce calcium waves, but it progresses for some time. In the meantime, the distortion wave for the outer black ring is terminated, but after an interval, a new distortion wave for the inner black ring is released. At this point, calcium wave induction and its self-enhancement occur, and inhibitory signals are produced at the wave edges, which finalize the position of the black rings. Genome amplification and the expression of regulatory genes follow. Cellular size increases at the prospective black rings according to the number of genomes in a cell. Where the calcium oscillations by self-enhancement are highly active, the high degree of cellular size increase occurs, resulting in the formation of a secondary organizing center, which is often seen in PFEs. This second round of color pattern determination ensures self-similarity between the eyespot and PFE.

In this series of events, the three most important events are distortion waves (D), calcium waves (C), and gene expression changes (G), which may be called the **DCG cycle**. This series of events repeats twice to create the self-similarity between the eyespot and PFE.

7.7.2 Generalization to Other Systems

Thus far, I have discussed the nymphalid wing color pattern system. The applicability of the information above to other butterfly systems has not been examined, but the lycaenid system is probably similar because the symmetry rule and the core-paracore rule hold true, at least in the lycaenid central symmetry system (Iwata et al. 2013, 2015). The fish skin system is different from the butterfly wing system in that epidermal cells in fish can move in response to surrounding cells, whereas butterfly cells cannot move. Nonetheless, the inductive nature of different colors based on short-range activation and long-range inhibition is likely shared in fish and butterflies; both systems can produce ectopic patterns associated with calcium waves after physical damage (Ohno and Otaki 2012).

Morphogenesis is three-dimensionally dynamic in any developmental system, but a good example of three-dimensional dynamism of the epithelial sheet is the morphogenetic furrow in the *Drosophila* retina (Greenwood and Struhl 1999; Schlichting and Dahmann 2008; Sato et al. 2013). The furrow is a physical distortion of the imaginal eye disk. This epithelial fold moves, and its movement coincides with cellular differentiation. The furrow may physically elicit the expression of morphogenetic genes such as *hedgehog* and *decapentaplegic* if the furrow is not a physical by-product of cellular differentiation.

7.7.3 DCG Cycle for Self-Similarity and Its Implications

Nearly two-dimensional butterfly wing color patterns can be viewed, somewhat ironically, as a developmental and evolutionary application of three-dimensional bulges and dents that are used in general morphogenesis. To achieve self-similar structures, organisms evolve to transmit a signal from the primary to secondary organizing centers through distortion waves of the epithelial sheet. This mechanical lateral signaling mechanism can cover a long distance with simplicity. Thus, it may be a very early evolutionary innovation. Evolution of the signal translator, mechanosensory calcium channels, might have followed, together with several genes that stabilize calcium oscillations and inhibition. In conclusion, the DCG cycle for self-similar structures has deep implications for biological evolution and development.

References

Adhikari K, Otaki JM (2016) A single-wing removal methods to assess correspondence between gene expression and phenotype in butterflies: a case of *Distal-less*. Zool Sci 33:13–20

Antunes M, Pereira T, Cordeiro JV, Almeida L, Jacinto A (2013) Coordinated waves of actomyosin flow and apical cell constriction immediately after wounding. J Cell Biol 202:365–379

Ball P (1999) The self-made tapestry: pattern formation in nature. Oxford University Press, Oxford

Ball P (2016) Patterns in nature: why the natural world looks the way it does. The University of Chicago Press, Chicago

Barnsley MF, Ervin V, Hardin D, Lancaster J (1986) Solution of an inverse problem for fractals and other sets. Proc Natl Acad Sci U S A 83:1975–1977

Beldade P, Koops K, Brakefield PM (2002) Modularity, individuality, and evo-devo in butterfly wings. Proc Natl Acad Sci U S A 99:14262–14267

Beldade P, French V, Brakefield PM (2008) Developmental and genetic mechanisms for evolutionary diversification of serial repeats: eyespot size in *Bicyclus anynana* butterflies. J Exp Zool Mol Dev Evol 310B:191–201

Ben-Jacob E, Shochet O, Tenenbaum A, Cohen I, Czirok A, Vicsek T (1994) Generic modelling of cooperative growth patterns in bacterial colonies. Nature 368:46–49

Brakefield PM, French V (1995) Eyespot development on butterfly wings: the epidermal response to damage. Dev Biol 168:98–111

Cho EH, Nijhout HF (2013) Development of polyploidy of scale-building cells in the wings of *Manduca sexta*. Arthropod Struct Dev 42:37–46

Dhungel B, Otaki JM (2009) Local pharmacological effects of tungstate in the color-pattern determination of butterfly wings: a possible relationship between the eyespot and parafocal element. Zool Sci 26:758–764

Dhungel B, Otaki JM (2013) Morphometric analysis of nymphalid butterfly wings: number, size and arrangement of scales, and their implications for tissue-size determination. Entomol Sci 17:207–218

Dhungel B, Ohno Y, Matayoshi R, Iwasaki M, Taira W, Adhikari K, Gurung R, Otaki JM (2016) Distal-less induces elemental color patterns in *Junonia* butterfly wings. Zool Lett 2:4

Family F, Masters BR, Platt DE (1989) Fractal pattern formation in human retinal vessels. Physica D: Nonlinear Phenomena 38:98–103

French V, Brakefield PM (1992) The development of eyespot patterns on butterfly wings: morphogen sources or sinks? Development 116:103–109

French V, Brakefield PM (1995) Eyespot development on butterfly wings: the focal signal. Dev Biol 168:112–123

Gierer A, Meinhardt H (1972) A theory of biological pattern formation. Kybernetik 12:30–39

Gilbert LE, Forrest HS, Schultz TD, Harvey DJ (1988) Correlations of ultrastructure and pigmentation suggest how genes control development of wing scales of *Heliconius* butterflies. J Res Lepidoptera 26:141–160

Greenwood S, Struhl G (1999) Progression of the morphogenetic furrow in the *Drosophila* eye: the roles of Hedgehog, Decapentaplegic and the Raf pathway. Development 126:5795–5808

Henke K (1946) Ueber die verschiedenen Zellteilungsvorgänge in der Entwicklung des beschuppten Flügelepithelis der Mehlmotte *Ephestina kühniella* Z. Biol Zentralbl 65:120–135

Henke K, Pohley H-J (1952) Differentielle Zellteilungen und Polyploidie bei der Schuppenbildung der Mehlmotte *Ephestia kühniella* Z. Z Naturforsch B 7:65–79

Hillyard SD, Willumsen NJ, Marrero MB (2010) Stretch-activated cation channel from larval bullfrog skin. J Exp Biol 213:1782–1787

Hiyama A, Taira W, Otaki JM (2012) Color-pattern evolution in response to environmental stress in butterflies. Front Genet 3:15

Iskratsch T, Wolfenson H, Sheetz MP (2014) Appreciating force and shape – the rise of mechanotransduction in cell biology. Nat Rev Mol Cell Biol 15:825–833

Iwasaki M, Ohno Y, Otaki JM (2017) Butterfly eyespot organizer: *in vivo* imaging of the prospective focal cells in pupal wing tissues. Sci Rep 7:40705

Iwata M, Otaki JM (2016a) Focusing on butterfly eyespot focus: uncoupling of white spots from eyespot bodies in nymphalid butterflies. SpringerPlus 5:1287

Iwata M, Otaki JM (2016b) Spatial patterns of correlated scale size and scale color in relation to color pattern elements in butterfly wings. J Insect Physiol 85:32–45

Iwata M, Hiyama A, Otaki JM (2013) System-dependent regulations of colour-pattern development: a mutagenesis study of the pale grass blue butterfly. Sci Rep 3:2379

Iwata M, Ohno Y, Otaki JM (2014) Real-time *in vivo* imaging of butterfly wing development: revealing the cellular dynamics of the pupal wing tissue. PLoS One 9:e89500

Iwata M, Taira W, Hiyama A, Otaki JM (2015) The lycaenid central symmetry system: color pattern analysis of the pale grass blue butterfly *Zizeeria maha*. Zool Sci 32:233–239

Janssen JM, Monteiro A, Brakefield PM (2001) Correlations between scale structure and pigmentation in butterfly wings. Evol Dev 3:415–423

Kaandorp JA, Kübler JE (2001) The algorithmic beauty of seaweeds, sponges, and corals. Springer, Berlin

Kazama M, Ichinei M, Endo S, Iwata M, Hino A, Otaki JM (2017) Species-dependent microarchitectural traits of iridescent scales in the triad taxa of Ornithoptera birdwing butterflies. Entomol Sci 20:255–269

Kohn AD, Moon RT (2005) Wnt and calcium signaling: β-Catenin-independent pathways. Cell Calcium 38:439–446

Kristensen NP, Simonsen TJ (2003) Hairs and scales. In: Kristensen PN (Ed). Lepidoptera, moths and butterflies: morphology, physiology, and development. Handbook of zoology, arthropoda: insecta, vol IV. Walter de Gruyter, Berlin, pp 9–22

Kühl M, Sheldahl LC, Park M, Miller JR, Moon RT (2000) The Wnt/Ca^{2+} pathway: a new vertebrate Wnt signaling pathway takes shape. Trends Genet 16:279–283

Kusaba K, Otaki JM (2009) Positional dependence of scale size and shape in butterfly wings: wing-wide phenotypic coordination of color-pattern elements and background. J Insect Physiol 55:174–182

Lee J, Ishihara A, Oxford G, Johnson B, Jacobson K (1999) Regulation of cell movement is mediated by stretch-activated calcium channels. Nature 400:382–386

Mahdi SHA, Gima S, Tomita Y, Yamasaki H, Otaki JM (2010) Physiological characterization of the cold-shock-induced humoral factor for wing color-pattern changes in butterflies. J Insect Physiol 56:1022–1031

Mahdi SHA, Yamasaki H, Otaki JM (2011) Heat-shock-induced color-pattern changes of the blue pansy butterfly *Junonia orithya*: physiological and evolutionary implications. J Therm Biol 36:312–321

Mandelbroit BB (1983) The fractal geometry of nature, Revised edn. W. H. Freeman, New York

Martin A, Reed RD (2014) *Wnt* signaling underlies evolution and development of the butterfly wing pattern symmetry systems. Dev Biol 395:367–378

Meinhardt H (1982) Models of biological pattern formation. Academic Press, London

Meinhardt H (2009) The algorithmic beauty of sea shells, Fourth edn. Springer, New York

Meinhardt H, Gierer A (1974) Applications of a theory of biological pattern formation based on lateral inhibition. J Cell Sci 15:321–346

Meinhardt H, Gierer A (2000) Pattern formation by local self-activation and lateral inhibition. BioEssays 22:753–760

Monteiro A (2008) Alternative models for the evolution of eyespots and of serial homology on lepidopteran wings. BioEssays 30:358–366

Monteiro A (2014) Origin, development, and evolution of butterfly eyespots. Annu Rev Entomol 60:253–271

Monteiro A, French V, Smit G, Brakefield PM, Metz JA (2001) Butterfly eyespot patterns: evidence for specification by a morphogen diffusion gradient. Acta Biotheor 49:77–88

Monteiro A, Prijs J, Bax M, Hakkaart T, Brakefield PM (2003) Mutants highlight the modular control of butterfly eyespot patterns. Evol Dev 5:180–187

Monteiro A, Glaser G, Stockslager S, Glansdorp N, Ramos D (2006) Comparative insights into questions of lepidopteran wing pattern homology. BMC Dev Biol 6:52

Monteiro A, Chen B, Ramos D, Oliver JC, Tong X, Guo M, Wang W-K, Fazzino L, Kamal F (2013) *Distal-less* regulates eyespot patterns and melanization in *Bicyclus* butterflies. J Exp Zool B Mol Dev Evol 320:321–331

Nadeau N, Pardo-Diaz C, Whibley A, Supple MA, Saenko SV, Wallbank RWR, Wu GC, Maroja L, Ferguson L, Hanly JJ, Hines H, Salazar C, Merrill RM, Dowling AJ, French-Constant RH, Laurens V, Joron M, WO MM, Jiggins CD (2016) The gene *cortex* controls mimicry and crypsis in butterflies and moths. Nature 534:106–110

Nijhout HF (1978) Wing pattern formation in lepidoptera: a model. J Exp Zool 206:119–136

Nijhout HF (1980a) Pattern formation on lepidopteran wings: determination of an eyespot. Dev Biol 80:267–274

Nijhout HF (1980b) Ontogeny of the color pattern on the wings of *Precis coenia* (Lepidoptera: Nymphalidae). Dev Biol 80:275–288

Nijhout HF (1981) The color patterns of butterflies and moths. Sci Am 254:145–151

Nijhout HF (1984) Colour pattern modification by coldshock in Lepidoptera. J Embryol Exp Morphol 81:287–305

Nijhout HF (1985) Cautery-induced colour patterns in *Precis coenia* (Lepidoptera: Nymphalidae). J Embryol Exp Morpholog 86:191–203

Nijhout HF (1990) A comprehensive model for color pattern formation in butterflies. Proc R Soc Lond B 239:81–113

Nijhout HF (1991) The development and evolution of butterfly wing patterns. Smithsonian Institution Press, Washington, DC

Nijhout HF (1994) Symmetry systems and compartments in Lepidopteran wings: the evolution of a patterning mechanism. Development 1994(Suppl):225–233

Nijhout HF (2001) Elements of butterfly wing patterns. J Exp Zool 291:213–225

Ohno Y, Otaki JM (2012) Eyespot colour pattern determination by serial induction in fish: mechanistic convergence with butterfly eyespots. Sci Rep 2:290

Ohno Y, Otaki JM (2015a) Live cell imaging of butterfly pupal and larval wings *in vivo*. PLoS One 10:e0128332

Ohno Y, Otaki JM (2015b) Spontaneous long-range calcium waves in developing butterfly wings. BMC Dev Biol 15:17

O'Neil RG, Heller S (2005) The mechanosensitive nature of TRPV channels. Pflugers Arch 451:193–203

Otaki JM (1998) Color-pattern modifications of butterfly wings induced by transfusion and oxyanions. J Insect Physiol 44:1181–1190

Otaki JM (2007) Reversed type of color-pattern modifications of butterfly wings: a physiological mechanism of wing-wide color-pattern determination. J Insect Physiol 53:526–537

Otaki JM (2008a) Physiologically induced color-pattern changes in butterfly wings: mechanistic and evolutionary implications. J Insect Physiol 54:1099–1112

Otaki JM (2008b) Phenotypic plasticity of wing color patterns revealed by temperature and chemical applications in a nymphalid butterfly *Vanessa indica*. J Therm Biol 33:128–139

Otaki JM (2008c) Physiological side-effect model for diversification of non-functional or neutral traits: a possible evolutionary history of *Vanessa* butterflies (Lepidoptera, Nymphalidae). Trans Lepid Soc Jpn 59:87–102

Otaki JM (2009) Color-pattern analysis of parafocal elements in butterfly wings. Entomol Sci 12:74–83

Otaki JM (2011a) Generation of butterfly wing eyespot patterns: a model for morphological determination of eyespot and parafocal element. Zool Sci 28:817–827

Otaki JM (2011b) Color-pattern analysis of eyespots in butterfly wings: a critical examination of morphogen gradient models. Zool Sci 28:403–413

Otaki JM (2011c) Artificially induced changes of butterfly wing colour patterns: dynamic signal interactions in eyespot development. Sci Rep 1:111

Otaki JM (2012a) Colour pattern analysis of nymphalid butterfly wings: revision of the nymphalid groundplan. Zool Sci 29:568–576

Otaki JM (2012b) Structural analysis of eyespots: dynamics of morphogenic signals that govern elemental positions in butterfly wings. BMC Syst Biol 6:17

Otaki JM, Yamamoto H (2004a) Species-specific color-pattern modifications of butterfly wings. Develop Growth Differ 46:1–14

Otaki JM, Yamamoto H (2004b) Color-pattern modifications and speciation in butterflies of the genus *Vanessa* and its related genera *Cynthia* and *Bassaris*. Zool Sci 21:967–976

Otaki JM, Ogasawara T, Yamamoto H (2005a) Morphological comparison of pupal wing cuticle patterns in butterflies. Zool Sci 22:21–34

Otaki JM, Ogasawara T, Yamamoto H (2005b) Tungstate-induced color-pattern modifications of butterfly wings are independent of stress response and ecdysteroid effect. Zool Sci 22:635–644

Otaki JM, Kimura Y, Yamamoto H (2006) Molecular phylogeny and color-pattern evolution of *Vanessa* butterflies (Lepidoptera, Nymphalidae). Trans Lepid Soc Jpn 57:359–370

Otaki JM, Hiyama A, Iwata M, Kudo T (2010) Phenotypic plasticity in the range-margin population of the lycaenid butterfly *Zizeeria maha*. BMC Evol Biol 10:252

Sato M, Suzuki T, Nakai Y (2013) Waves of differentiation in the fly visual system. Dev Biol 380:1–11

Schlichting K, Dahmann C (2008) Hedgehog and Dpp signaling induce cadherin Cad86C expression in the morphogenetic furrow during *Drosophila* eye development. Mech Dev 125:712–728

Schwanwitsch BN (1924) On the ground plan of wing-pattern in nymphalid and certain other families of rhopalocerous Lepidoptera. Proc Zool Soc London 34:509–528

Serfas MS, Carroll SB (2005) Pharmacologic approaches to butterfly wing patterning: sulfated polysaccharides mimic or antagonize cold shock and alter the interpretation of gradients of positional information. Dev Biol 287:416–424

Simonsen TJ, Kristensen NP (2003) Scale length/wing length correlation in Lepidoptera (Insecta). J Nat Hist 37:673–679

Sondhi KH (1963) The biological foundations of animal patterns. Q Rev Biol 38:289–327

Süffert F (1927) Zur vergleichende Analyse der Schmetterlingsaeinchnung. Biol Zentralbl 47:385–413

Taira W, Otaki JM (2016) Butterfly wings are three-dimensional: pupal cuticle focal spots and their associated structures in *Junonia* butterflies. PLoS One 11:e0146348

Taira W, Kinjo S, Otaki JM (2015) The marginal band system in the nymphalid butterfly wings. Zool Sci 32:38–46

Teng X, Toyama Y (2011) Apoptotic force: active mechanical function of cell death during morphogenesis. Dev Growth Differ 53:269–276

Toyama Y, Peralta XG, Wells AR, Kiehart DP, Edwards GS (2008) Apoptotic force and tissue dynamics during *Drosophila* embryogenesis. Science 321:1683–1686

Tracey WD Jr, Wilson RI, Laurent G, Benzer S (2003) *painless*, a *Drosophila* gene essential for nociception. Cell 113:261–273

van't Hof AE, Campagne P, Rigden DJ, Yung CJ, Lingley J, Quail MA, Hall N, Darby AC, Saccheri IJ (2016) The industrial melanism mutation in British peppered moths is a transposable element. Nature 534:102–105

Zhang L, Reed RD (2016) Genome editing in butterflies reveals that *spalt* promotes and *Distal-less* represses eyespot colour patterns. Nat Commun 7:11760